

## ***CHAPTER 3***

### ***PVA/Chitosan Lactate Composite Hydrogel***

### **3. Polyvinyl Alcohol/Chitosan Lactate Composite Hydrogel for Controlled Drug Delivery**

The aim of the present chapter was to develop composite hydrogel and its evaluation, as a drug delivery matrix, for sustained release of hydrophilic drugs. Composite drug-loaded hydrogels were prepared by blending of chitosan lactate with polyvinyl alcohol followed by cross-linking with glutaraldehyde. This has been further characterized by Fourier transform infrared (FTIR) spectroscopy and X-ray diffraction. The developed PVA/Chitosan Lactate (PVA/CL) based hydrogels were cross-linked in order to enhance its physico-chemical properties. Freezing bound water was measured by differential scanning Calorimetry (DSC) to analyze the cold crystallization characteristics of the hydrogel. The cell cytotoxicity and drug release properties of PVA/CL hydrogels membrane was also investigated. *In vitro* cell viability of L929 cells shows that the fabricated hydrogels are compatible with cells and facilitate cells adhesion. Moreover, the sustained release of ciprofloxacin from developed drug-loaded hydrogels inhibits the growth of *E. coli* and thus facilitates antimicrobial activity under physiological condition. Thus, we anticipate the improved properties of the fabricated composite hydrogels might be suitable for controlled drug delivery, anti-infective coatings, and wound dressing.

#### **3.1 Introduction**

Three-dimensional networks of hydrophilic polymers in hydrogels attracted attention towards the incorporation of a higher number of drugs for their application in slow, sustained and controlled drug delivery due to formation of covalent bonds, ionic interaction, hydrogen bonding and hydrophobic interactions[104-109]. Over the last few decades, natural and synthetic polymer- based hydrogels have been developed for

sustained drug release applications[110, 111]. Although the natural polymers exhibit high biocompatibility and biodegradability as compared to synthetic polymer[112], both along with, their blends have been reported. For instance, cross-linked hydrophilic gels of poly(2-hydroxyethyl methacrylate) (PHEMA) for permanent contact lenses[113], papain wound dressings obtained from poly(vinyl alcohol)/calcium blends[114]polyvinyl alcohol/cellulose cryogels as carriers for a bioactive component[115], chitosan hydrogel for protein sorption[108]and many more.Paduraru et al. have conferred physical hydrogel-based formulations as a carrier for bioactive compounds. These carriers may be accepted as a drug delivery matrix. But due to its poor mechanical strength, it can be used for a shorter duration only. In the case of an extended period, this matrix will be degraded due to its poor crosslinking network. This is the major problem observed with the physical hydrogel-based drug delivery matrix[116]. Among various natural and synthetic polymers, PVA and chitosan were used widely to develop hydrogel for biomedical application.

Chitosan is a most abundant linear polysaccharide after cellulose. It comprises of  $\beta$ -(1-4)-linked D-glucosamine and N-acetyl-D-glucosamine units in random fashion[108]. Its non-toxicity, antimicrobial and bioactivity properties[117] have attracted extensive applications in the area of biomedical engineering field. Assaadet et al. reported injectable high strength thermoresponsive hydrogels, which used salt with buffer[118]. Whereas, Xu et al. developed catechol- chitosan mucoadhesive hydrogels for buccal cavity drug release[119], Hu et al. developed methacrylated glycol Chitosan through the visible light crosslinking process for cartilage tissue engineering applications.Hu et al. have evolved Glycol Chitosan-based hydrogel using the visible light crosslinking method. Although Glycol Chitosan is a water-soluble derivative of Chitosan, its huge price may restrict its wide applications[120]. But the major problem associated with the

photo crosslinking method is the optimization of photo initiator concentration and radiation intensity. Inappropriate selection of these parameters may lead to poor mechanical strength[121]. Whereas the uses of chitosan lactate, a water-soluble Chitosan derivative is expected to provide more biocompatibility due to eliminating the acid solubilization step. This will also result in the development of a mechanically more stable hydrogel system due to chemical crosslinking. Besides chitosan lactate is less expensive. To improve the biocompatibility, cost-effectiveness and versatility of hydrogel, we need to develop a new hydrogel system with enhanced properties.

Earlier authors have also reported generation of hydrogel using blends of PVA and chitosan using gamma radiation. These hydrogels are biocompatible with fibroblast[122]. Anamarija et al. prepared physically crosslinked chitosan-hydroxyapatite hydrogel with sodium bicarbonate by reducing the acidity of chitosan solution, for application as a cell carrier[123]. Whereas, chitosan/ $\alpha\beta$ -GP was produced by dissolving chitosan in acetic acid/sodium acetate buffer solution and using adriamycin as binder. Developed polymers was used in cancer chemotherapy[124]. On the other hand, Yingchun et al. developed a chitosan-based thermosensitive hydrogel, with high mechanical strength for intratumoral delivery of paclitaxel[125]. Fereshteh et al. developed degummed silk fibers reinforced thermosensitive chitosan hydrogels for hyaline cartilage regeneration[126].

In some reports, acidic medium was used to completely dissolve chitosan for the formation of chitosan-based hydrogel. The developed hydrogel caused serious problems in different biological applications[127, 128]. A significant study by Sogias et al., 2010, clearly states that Chitosan shows solubility in solvent possess  $\text{pH} < 6$ . Acid solubilized Chitosan undergoes precipitation upon raising the pH of the solvent more than 6. It does not allow complete removal of acidic residues and hence only way out is to develop a

water-soluble chitosan derivative[100].Further, Zhou et al. reported that residual acid present in the final product might damage tissue or wound. They have used Chitosan in their work and dissolved it using acrylic acid, followed by neutralization using Sodium hydroxide to get sodium salt[129].Therefore, in the present work, chitosan lactate (CL), derived from water soluble chitosan has been used to develop a novel hydrogel membrane. Developed hydrogel did not use acidic solvents and was cross-linked by glutaraldehyde. Glutaraldehyde is known to be used in applications such as that bioprosthetic implants. On the other hand, acid remaining in the chitosan hydrogel leads to hydrogel's shrinkage upon shifting to Solvent having pH 7.4 [130]. Therefore, glutaraldehyde is safer for biological application than acid. Obtained crystalline structures and chemical properties were evaluated using X-ray diffractometer and FT-IR spectroscopy. The surface topology of the hydrogel membranes was investigated using scanning electron microscopy (SEM) and atomic force microscopy (AFM). Whereas its antibacterial activity was examined by a gram-negative bacterium. Antibacterial studies were performed using hydrogel with and without loading antibacterial drugs. Prior to antibacterial activity, biocompatibility of these hydrogel was also demonstrated by performing cell viability and proliferation assay using L929 cell line.

### **3.2 Materials and Methods**

Polyvinyl alcohol (Molecular Weight 1,15,000, Hydrolysis 99%), glutaraldehyde and hydrochloric acid was purchased from LobaChemie India, Chitosan Lactate (average degree of deacetylation: 90%) was procured from Everest Biotech, Bengaluru, India. Ciprofloxacin hydrochloride was purchased from Sisco Research Laboratories, India.

### 3.3 Preparation of Hydrogel

Polyvinyl alcohol aqueous solution (10% w/w) was prepared by autoclaving at 121°C for 1 hour. Similarly, different concentration of chitosan lactate aqueous solution (0.25% w/w, 0.50% w/w, 1% w/w, and 2% w/w) was prepared by above method. Glutaraldehyde reagent was prepared by diluting 5 mL of glutaraldehyde (25% w/w) in 10 mL of ethyl alcohol. Five hydrogel compositions were made by mixing 18 g of 10% (w/w) PVA solution, 20 mL water and 2 g of water (PVA/CL-1) or, 2 g of chitosan lactate solutions of different concentrations (0.25, 0.50, 1, and 2 %, w/w) (PVA/CL-2, PVA/CL-3, PVA/CL-4, and PVA/CL-5, respectively). Under continuous stirring at 60 rpm for 10 min at room temperature (RT= 27°C). To each composition, 1 mL glutaraldehyde reagent cross-linker was then added, under moderate stirring for 30 min. Then, 20 grams of resultant solutions was cast into polystyrene petri dishes (internal diameter 8.5 cm) and kept for 20 min at ambient conditions, and finally transferred to an incubator maintained at 37°C and kept for 24 h. The hydrogel film (PVA/CL-1), without chitosan lactate, was treated as the control in this study. Thereafter, hydrogel thin films were obtained from the solution casting method and taken out from the Petri dishes, then dipped in distilled water for five days to remove un-reacted chemical residues. During this process, water was exchanged with fresh distilled water every 12 h. Purified films were dried under vacuum at room temperature for 12 h. To block the formed free aldehyde groups, these films were soaked in 0.1 M glycine solution for 1 h, followed by washing with distilled water and then with phosphate buffer solution (PBS) of pH 7.4[131]. Finally, hydrogels sheets were dried at room temperature using a vacuum oven for 12 h and kept in desiccators for further study.

### **3.4 Characterizations**

#### **3.4.1 Fourier transforms infra-red spectroscopy**

To quantify molecular interactions between the poly (vinyl alcohol) and chitosan lactate, Fourier Transform Infrared Study (FT-IR) was performed. The FTIR (AlphaE ATR-FTIR, Bruker, Germany spectroscopy was used to quantify molecular interactions of all the samples including synthetic polymer in powdered condition and hydrogel films prepared by solution casting technique. All of the FTIR spectra were obtained in the wavenumber ranging from 400 to 4000  $\text{cm}^{-1}$ .

#### **3.4.2 X-ray diffraction measurement**

To investigate crystallinity, X-ray diffraction measurements (XRD) was carried out by using Rigaku Miniflex 600 Desktop X-Ray Diffraction System. The data were recorded at  $2\theta$  ranging from  $10^0$  to  $60^0$ .

#### **3.4.3 Differential scanning calorimeter**

Differential scanning calorimetry was performed (DSC 200 F3, Maia, Netzsch, Germany) by taking small amount of (~9–13 mg) of each sample, and purging it with nitrogen gas.

#### **3.4.4 Thermogravimetric analysis**

Thermogravimetric analysis was performed on Perkin Elmer-STA 6000, in the temperature, ranging from 50  $^{\circ}\text{C}$  to 600  $^{\circ}\text{C}$ .

#### **3.4.5 Scanning electron microscopy**

Scanning Electron Microscopy (SEM) was used to understand the surface morphology of the hydrogel membrane. The developed hydrogel was analyzed by Scanning Electron Microscope (FEI QUANTA 450) at 4.00 K x magnification. Before SEM study, the hydrogel sheet was freeze dried for 24 hours followed by surface coating with gold.

### 3.4.6 Atomic force microscopy

Atomic Force Microscopy (AFM) was used for obtain 3D surface topology, and to get insight into surface roughness of the hydrogel membrane. The AFM study of all the membranes was performed at non-contact mode and average roughness value was estimated using Nova Software.

### 3.4.7 Swelling behavior

In order to understand the water holding capacity of the hydrogel, swelling of the hydrogel was performed using phosphate buffer (pH 7.4) at 37°C, after lyophilization. The swollen hydrogels were taken at a regular interval (30 min), and gently blotted with filter paper and weighed. The swelling index of hydrogel was calculated by the following equation (3.1) [132].

$$\text{Swelling Index} = \frac{W_t - W_o}{W_o} * 100 \quad (3.1)$$

where  $W_t$  is the weight of swollen hydrogel at specific time  $t$  and  $W_o$  is initial dry weight of hydrogel at start of the experiment.

### 3.4.8 In Vitro degradation study

To get insight into the stability of hydrogel network, in vitro degradation of all the prepared hydrogels were performed according to reported literature[133]. In vitro degradation study of hydrogels was performed in PBS (pH 7.4) at 37 °C. To perform degradation study, disc shaped hydrogel samples were dipped into 5 mL of PBS Solution for 2-hour, 6-hour, 12-hour, 24-hour, 48 hour and 96 hours. After certain period of time interval, wetted sample were dried in vacuum at 40 °C for 2 hour and weight was measured.



In Vitro degradation of hydrogels was calculated by following formula, (3.2)-

$$\text{Degradation Rate} = \frac{m_o - m_t}{m_o} \times 100 \quad (3.2)$$

where  $m_o$  and  $m_t$  are the weight of hydrogel disc at start of experiment and after time period  $t$ .

### 3.4.9 Mechanical study of hydrogel

To understand the mechanical property of the hydrogels, stress relaxation test of all the hydrogels were performed[128]. Mechanical study of these hydrogels was performed at 37 °C. Stress relaxation study was performed using static mechanical tester machine (TA HD –Plus, Stable Micro Systems, Haskmere, England). Hydrogel samples were cut into rectangular dimension of 60 mm × 5 mm. Sample was clamped in such a way that the effective sample length was 50 mm. During this study, stretching rate of 1 mm/ sec was applied to the sample upto 5 mm distance. Now sample was held at this condition upto 60 seconds to observe stress relaxation pattern of hydrogels.

### 3.4.10 Drug loading and release study

The drug was loaded to the prepared hydrogels, by swelling equilibrium method[134] via dipping of 1 cm x 1 cm hydrogel films in 20 mL of 0.2% (w/v) aqueous solution of Ciprofloxacin hydrochloride drug, for 24 h. To perform drug release study, drug-loaded hydrogel sheet was cut into a square shape (1cm×1cm) and kept inside the dialysis membrane (MWCO 12 kDa). These dialysis membranes were dipped in a beaker containing 20 mL phosphate buffer saline (PBS, pH 7.4) and subjected to continuous shaking at 37°C temperatures. Shaking is required to maintain uniform concentration throughout the drug-releasing medium. The shaking speed was kept at 100 rpm throughout the drug release study. It is a standard protocol followed to perform a drug release study from a drug-releasing device. It is not essential that hydrogel will encounter

a similar condition when it is used for clinical or therapeutic application. For example, if the drug-loaded hydrogel is used in the gastrointestinal route, it will experience shaking due to peristaltic movement. Whereas, when a drug delivery system is used for topical application as a skin implant, hydrogel will experience little shaking environment.

From this solution, a small aliquot (4 mL) was withdrawn at different time intervals to check its absorbance and replaced by the same volume of fresh PBS. The concentration of drug released was measured by UV Visible Spectrophotometer (Shimadzu, UV-1700 Pharma spec) at 270 nm. The drug release was quantified by comparing the calibration curve made by measuring the absorbance at 270 nm of the drug solutions of different concentrations in PBS. The cumulative release of ciprofloxacin from drug-loaded hydrogel was evaluated and the result was plotted over time.

#### 3.4.11 Drug loading efficiency evaluation

Drug loading efficiency of all the hydrogels were computed according to the reported literature with slight modification[89]. During the loading process, the temperature (37°C) and pH (7.4) of the loading medium were kept constant. The drug loading capacity of each hydrogel depends on the polymer network of developed hydrogel and its compactness. We can expect drug loading based on the hydrogel network and its composition. In order to study the drug loading efficiency, each hydrogel of dimension 1 cm<sup>2</sup> was dipped into 30 mL ciprofloxacin drug solution containing 21 mg of ciprofloxacin drug for 24 hours at temperature 37°C. After achieving equilibrium, hydrogel sample were blotted with filter paper and weight of each hydrogels were measured. After that, drug loading efficiency of all the hydrogels were measured using following formula (3.3)

$$\text{Ciprofloxacin loading Efficiency (\%)} = \left[ \frac{(m_2 - m_1) \times (0.7/1000)}{m_1} \times 100 \right] \quad (3.3)$$

where  $m_1$  and  $m_2$  are the weight of dry and swollen hydrogels, respectively.

When a blank hydrogel (without drug) is placed in drug loading solutions of specific pH, hydrogel swelling occurs. During the process of swelling, not only movement of solvent (water) along with the drug occurs into the hydrogel, but also diffusion of the drug into the pores of hydrogel occurs. The swelling process terminates when equilibrium is established between the hydrogel and drug loading solution. Upon termination of swelling, the movement of the drug into the hydrogel occurs through diffusion only. Therefore, it can be concluded that the movement of drugs into hydrogel occurs through both convective transport of water-loaded drugs and diffusion of drugs[135].

#### **3.4.12 Antimicrobial evaluation**

The antimicrobial activity of hydrogels was performed by Agar Disc diffusion method, using common bacteria *E. coli* according to the available reported literature with some modification[125]. For sterilization of agar, steam pressure should be 15 pound (lbs) per square inch for 30 minutes. This medium was transferred to sterilized polystyrene petri dish (Tarson) for solidification. After solidification of agar media, *E. coli* culture (100  $\mu$ L of *E. coli* suspension of  $1 \times 10^6$  CFU/mL) was spread over the surface of solidified agar. To this inoculated petri dish, test sample, blank sample, and control sample were placed and subjected to incubation for 2 days at 37 °C. Hydrogel loaded with ciprofloxacin drug was considered as a test sample and it was designated as positive, whereas hydrogel without drug was considered as blank Sample and it was designated as negative. Disc-shaped Filter paper saturated with ciprofloxacin drug (drug concentration-1mg/mL) was considered a control sample. After 2 days zone of inhibition formed around samples was measured.

### **3.4.13 Contact angle evaluation**

Contact angle of all the hydrogels were determined by Kruss F-100 tensiometer system using water as test fluid. Before performing this test, length, width and thickness of each sample was measured. To estimate the hydrophilic or hydrophobic behavior of the hydrogel, contact angle measurements were performed.

### **3.4.14 Cell culture studies**

Mouse originated fibroblast-like NCTC clone L929 cell line procured from National Centre for Cell Science (NCCS), Pune, India. The cells were cultured in Dulbecco's modified Eagle's medium (DMEM) supplemented with 10% heat-inactivated fetal bovine serum (Himedia, Mumbai, India), penicillin (100U/mL) and streptomycin (100 microgram/mL). These cells were maintained at 37 °C using humidified incubator with 5% CO<sub>2</sub>. The hydrogel films were washed properly using 1 mM PBS and kept 24 h in 70% ethanol for sterilization. The washed and sterilized hydrogel films were cut into a square sheet of 3×3 mm<sup>2</sup> and released into well of tissue culture plate in triplicate. Separately, L929 cells were seeded into 96 well tissue culture plate with hydrogels and without hydrogel (used as a control) at a density of  $1 \times 10^4$  cells per well and the culture media were maintained at 200 µl in each well. After 24 h, cultured cells were washed twice with 1 mM PBS to remove the dead cells along with cell debris and 200 µl fresh culture media were maintained. These cells seeded tissue culture plates (with and without hydrogels) in triplicate were incubated further for 24, 48 and 72 h respectively.

### **3.4.15 Cell viability**

To measure the cell viability at 24 h and cell proliferation at day 2 and day 3, MTT assay performed. MTT assay is the spectroscopic measurement of conversion of yellow-colored tetrazolium salt to purple formazan crystal by the mitochondrial enzymes of the active

cell. After incubation, the culture media and sheets were removed from the well and 100  $\mu$ l of MTT solution containing 0.5 mg/mL MTT in culture media without PBS was added and further incubated for 4 h at 37 °C. 100  $\mu$ l of DMSO was added in each well to dissolve MTT formazan crystals and finally, absorbance was measured at 570 nm using a microplate ELISA plate reader.

#### **3.4.16 EtBr/AO staining**

Fluorescence microscopy was performed to detect quantitative estimation of live and dead cells. The L929 the cell line was used which was suspended in fresh medium at a density of  $1 \times 10^4$  cells per mL and seeded into 24 well plates. After 24 h of incubation, the old medium was replaced with fresh medium in each well and the sheets were released into the well in triplicate which was further incubated for 24 h. Then, washing of cells have been done by PBS and was stained with fluorescent dye acridine orange and ethidium bromide at a concentration of 100  $\mu$ g/ mL each. After that, cells were subjected to incubation in dark place for the next 30 min at room temperature. Images of cells were obtained by a fluorescence microscope (Dewinter Technologies, India).

#### **3.4.17 Statistics studies**

Statistical analyses were performed using GRAPH PAD PRISM for window software. The results were presented as mean values. Cell viability data were analyzed using Dunnett's method for several comparative tests in ANOVA. p values were obtained from ANOVA analysis and the conventional value (0.05) was considered to represent statistical significance. Each experiment was repeated three times.

### **3.5 Result and Discussion**

#### **3.5.1 Physico-chemical characterization**

A schematic representation of possible chemical interaction between polyvinyl alcohol and chitosan lactate through glutaraldehyde as a crosslinker is shown in figure 3.1, which has been further evaluated by using various techniques such as FTIR, XRD and shown in Figures (3.2, 3.3). FTIR spectra of PVA hydrogel showed a wide peak from 3200 to 3700  $\text{cm}^{-1}$  of hydroxyl group due to the intramolecular and intermolecular hydrogen bonding. The peak in the range of 2898 to 2946  $\text{cm}^{-1}$  which is attributed to the C-H bond of the alkyl group, the band between 1700 and 1750  $\text{cm}^{-1}$  indicates stretching of C=O functional moieties of the acetate groups remaining in the PVA[136]. Yang et. al.[90], Hassan et. al.[137] reported the absorption peak around at 1142  $\text{cm}^{-1}$  of PVA gels crystallinity. Chitosan lactate shows the peak at 1557  $\text{cm}^{-1}$ , due to amino group of chitosan lactate. The Peak in the region 1500-1750  $\text{cm}^{-1}$  indicates the presence of amine and amide (both primary and secondary) and the peak in the range of 900-1200  $\text{cm}^{-1}$  due to the N-H wagging in out of the plane[138]. A thin sheet of polyvinyl alcohol-chitosan lactate composite hydrogel membrane at various concentrations of CL in PVA prepared and functional groups interactions were identified by FTIR. FTIR study of PVA/CL composite hydrogel clearly reveals the dominance of PVA over chitosan lactate. It may be due to the low concentration of chitosan lactate with respect to PVA in the resultant composite hydrogel. The broad peak at 3042-3601  $\text{cm}^{-1}$  was observed in all the cross-linked hydrogels which confirms the formation of a hydrogel[139]. The reaction between the hydroxyl group of PVA and CL reacts with the -CHO of glutaraldehyde, thus a peak around 1600-1700  $\text{cm}^{-1}$  was observed, which confirms the presence of ketonic functionality[140]. FTIR peaks of PVA/ CL composite hydrogels reflect the dominance of PVA over Chitosan Lactate. PVA shows some desirable properties such as stable structure and chemical inertness as well. Therefore, it has been considered safe to develop various drug release formulations[141]. Although, it shows less cell adhesion

property[142]. Therefore, it has been combined with Chitosan lactate to improve its biocompatibility. It will assist in fulfilling possible drug delivery application.

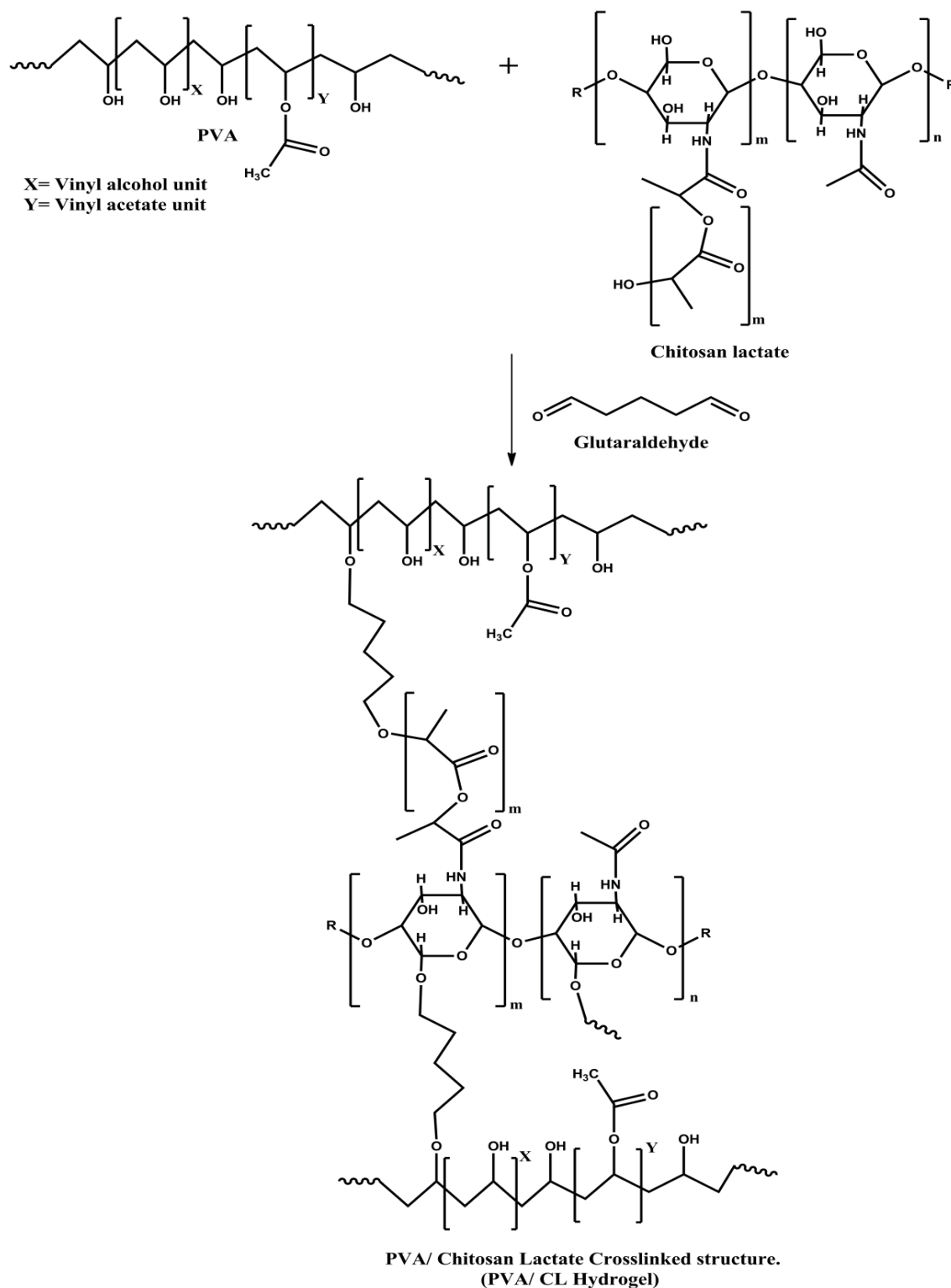


**Figure 3.1:** Proposed Mechanism of glutaraldehyde reaction with polyvinyl alcohol and chitosan lactate to form hydrogel.

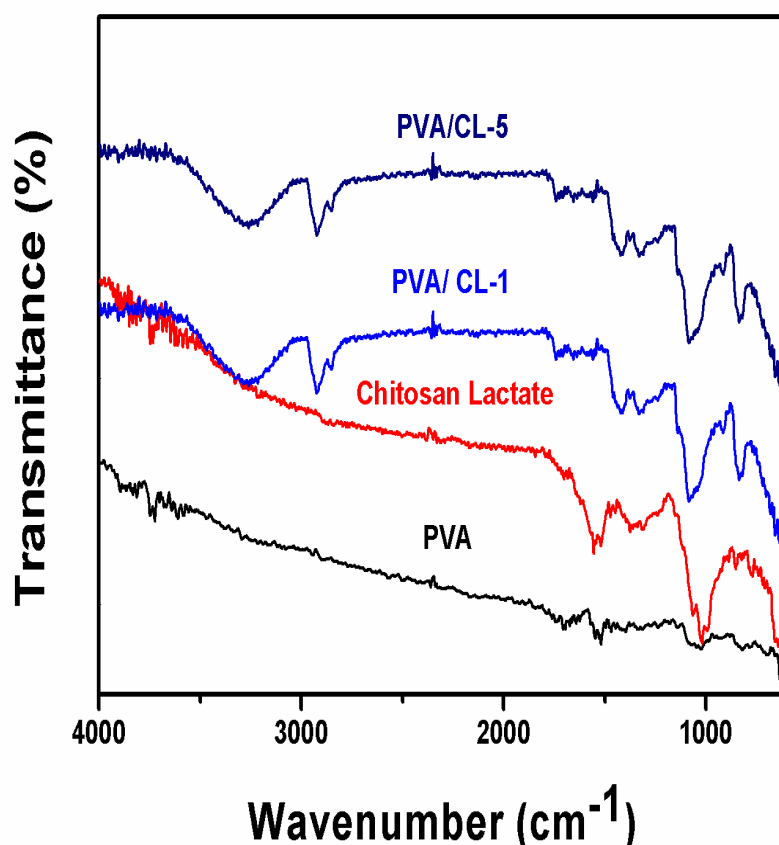


**Figure 3.2:** FTIR spectra of (i) PVA Powder (ii) chitosan lactate powder (iii) PVA/CL-1 hydrogel (iv) PVA/CL-5 hydrogel.

In addition to PVA exhibit major peaks characteristic of polymer crystallinity at  $19^\circ.35^\circ$ ,  $23.2^\circ$  and  $40.88^\circ$ . Chitosan exhibits two characteristic peaks, a hydrated crystalline moiety at around  $20$ ,  $18.6^\circ$  and a wide peak around  $23^\circ$  for amorphous structure[143]. The composite hydrogels prepared from PVA exhibited a major prominent peak at  $20.5^\circ$  and minor diffraction peak at approximately  $41^\circ$ . Interestingly, XRD spectra of hydrogel membrane PVA/CL-1 which have only PVA cross-linked with glutaraldehyde, shows that the appearance of a minor peak at around  $41^\circ$  decreases with the increase of chitosan lactate concentration. The disappearance of minor peak at  $41^\circ$  may be due to the strong interaction of the end terminal containing  $-OH$  group of CL and PVA with  $-CHO$  of glutaraldehyde or the CL molecule covers up the PVA by the efficient cross-linking. It is



important to note that crystallinity of resultant hydrogel has reduced (seen with the increase in full-width half maxima of the diffraction peak at  $20.5^\circ$  and disappearance of peak at  $41^\circ$ ) as a function of chitosan lactate concentration. The reduction in crystallinity of resultant hydrogels may be due to the interaction between polymer chains of polyvinyl alcohol and polymer chains of chitosan lactate resulting into formation of more amorphous regions[144-146].

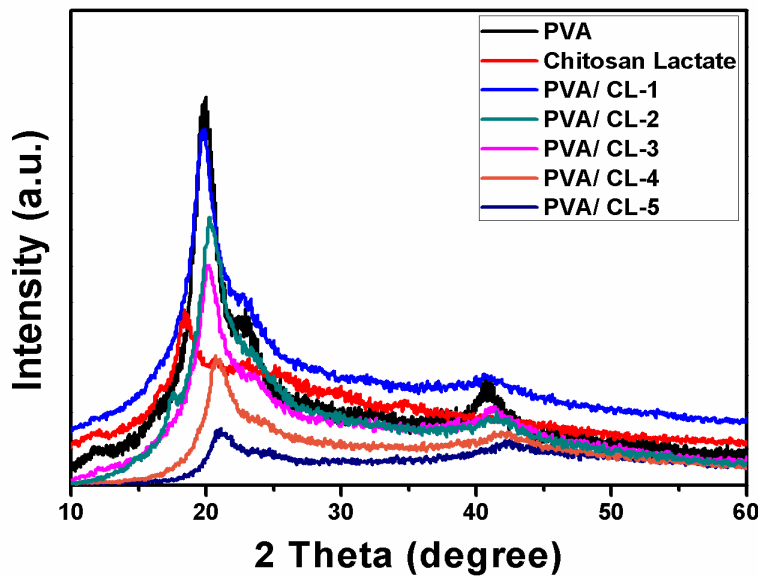


**Figure 3.3:** XRD spectra of (i) PVA Powder (ii) chitosan lactate powder (iii) PVA/CL-1 hydrogel (iv) PVA/CL-2 hydrogel (v) PVA/CL-3 hydrogel (vi) PVA/CL-4 hydrogel (vii) PVA/CL-5 hydrogel.

The scanning electron microscopy images presented very similar morphological aspects for the PVA/CL samples at different chitosan ratios, showing the formation of uniform and continuous films (Figure 3.4). The topology of hydrogels gradually changes with the addition of chitosan lactate. Hydrogel sample without chitosan lactate shows smoother surface with respect to composite hydrogels as shown in PVA/CL-1. The change in the topology of hydrogel due to the addition of chitosan lactate may be due to the phase

separation phenomenon; thus composite hydrogels show rougher surface. Wang et al. 2004 described that PVA and chitosan, prior to chemical cross-linking have their chains mostly, physically entangled in the hydrogel network, but formed a chemically bonded hydrogel after glutaraldehyde cross-linking has taken place[86]. The SEM images revealed very distinct change in the porous structure of the composite hydrogels on moving from PVA/CL-1 to PVA/CL-5. PVA/CL-1 micrographs show a shallow cross-linked polymeric network. Which becomes slightly deeper accompanied with formation of bigger polymeric islands and deeper pores in PVA/CL-2. Figure shows that as the CL amount is increased, the number of compact pores increases greatly. These pores become smaller in size and uniformly distributed in the compact solid polymer matrix of PVA/CL-3. Whereas in the case of PVA/CL-4 number of compact pores significantly increase in comparison to PVA/CL-1, PVA/CL-2 and PVA/CL-3. Also number of pores with bigger size decrease while small ones increase as compared to its previous counterparts. These changes clearly show that with the increase in chitosan lactate formation of compact and small pores increases finally making a compact PVA/CL-5 matrix.

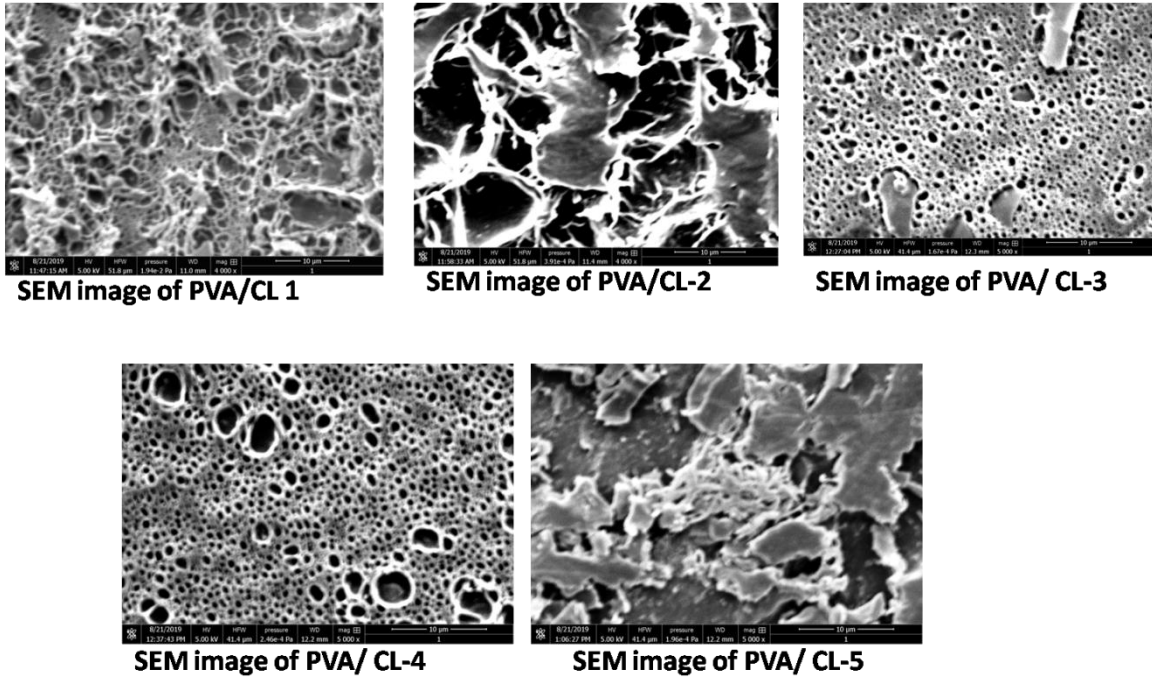


**Figure 3.4:** SEM image of (scale bar 10 µm)(i) PVA/CL-1 hydrogel(ii) PVA/CL-2 hydrogel (iii) PVA/CL-3 hydrogel (iv) PVA/CL-4 hydrogel (v) PVA/CL-5 hydrogel

AFM study (Figure 3.5) of all hydrogel samples was performed at 20 µm and average roughness value was calculated. The average roughness value was lowest 17.8 nm for PVA/ CL-2 hydrogel, whereas the highest average roughness value was, 160.3 nm observed for PVA/CL-5 hydrogel. From the AFM measurement study, it can be concluded that the roughness of hydrogel increases with the increase in chitosan lactate concentration.

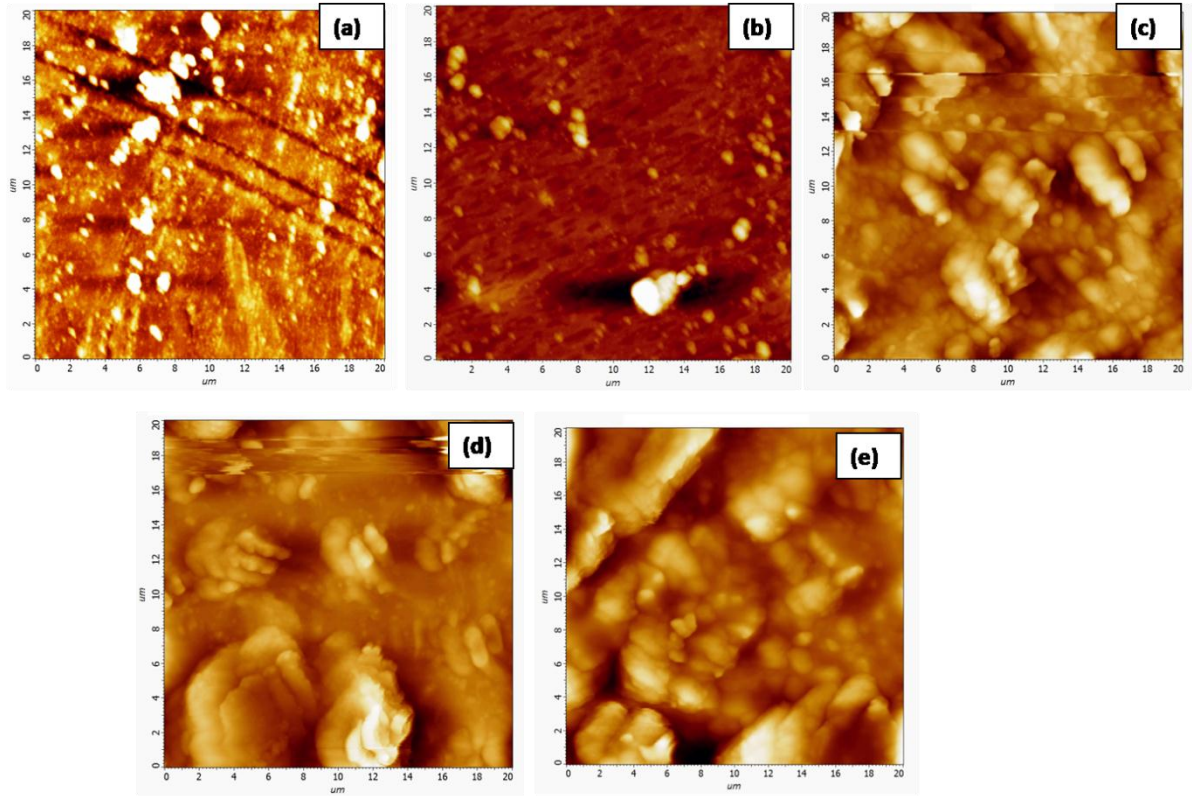


**Figure 3.5:** AFM image of (a) PVA/CL-1 hydrogel (b) PVA/CL-2 hydrogel (c) PVA/CL-3 hydrogel (d) PVA/CL-4 hydrogel (e) PVA/CL-5 hydrogel.

Figure (3.6 a) shows the DSC thermograms of the uniaxially drawn PVA, CL film and PVA/CL composite hydrogel membrane. PVA hydrogel without CL shows, sharp endothermic peak at around 222 °C whereas other hydrogels such as PVA/CL-3 and PVA/CL-5 showed an endothermic peak at around 214 °C and 207 °C, respectively. The Shifting of  $T_g$  for PVA/CL from 222 to 207 °C might be due to the strong binding of CL with PVA [90] after the glutaraldehyde treatment and presence of chitosan lactate, leading to increase in amorphous behavior of composite hydrogel[147]. This result was also supported by X-ray diffraction study of composite hydrogels. Figure (3.6 b) shows TGA analysis of developed hydrogel, in which PVA hydrogel shows weight loss in five stages first (6%) between 50 °C to 220 °C, second (22%) between 220 °C to 310 °C, third (38%) between 310 °C to 400 °C, fourth (25%) between 400 °C to

520 °C and fifth (4%) between 520 °C to 590 °C. PVA/CL hydrogel also shows weight loss in five stages first (5%) between 50 °C to 150 °C, second (61%) between 150 °C to 400 °C, third (8%) between 400 °C to 430 °C, fourth (~13%) between 430 °C to 530 °C and fifth (~2%) between 530 °C to 600 °C. Thus, the prepared hydrogel showed enhanced thermal stability with respect to PVA hydrogel. The better thermal stability is due to the active participation of glutaraldehyde with PVA and chitosan lactate, resulting in the formation of stable three-dimensional polymeric networks. The thermal stability of chitosan-PVA hydrogel membrane was enhanced by adding glutaraldehyde as cross-linker. Chitosan, is a linear polysaccharide, has been found to be a good chemical entity for synthesizing composite because of its greater cross-linking ability, due to the presence of (-NH<sub>2</sub>) amino group. This amino group and aldehyde group forms a Schiff's base reaction causing high thermal stability to blends[95]. From the DTGA graph (figure 3.7) of PVA/ CL-1, it is clear that the rate of thermal degradation is highest at temperature at 349.9°C. Whereas, the higher rate of thermal degradation for PVA/ CL-3 and PVA/ CL-5 hydrogels occurred at temperature 337.9°C and 342.8 °C respectively. It shows that PVA/ CL-1 hydrogel shows the rate of thermal degradation at higher temperature with respect to PVA/ CL-3 hydrogel and PVA/ CL-5 hydrogel. PVA/CL-5 hydrogel shows thermal degradation at higher temperature with respect to PVA/ CL-3 hydrogel. This enhancement in thermal degradation is may be due to formation of compact composite network and polymeric chain interaction.

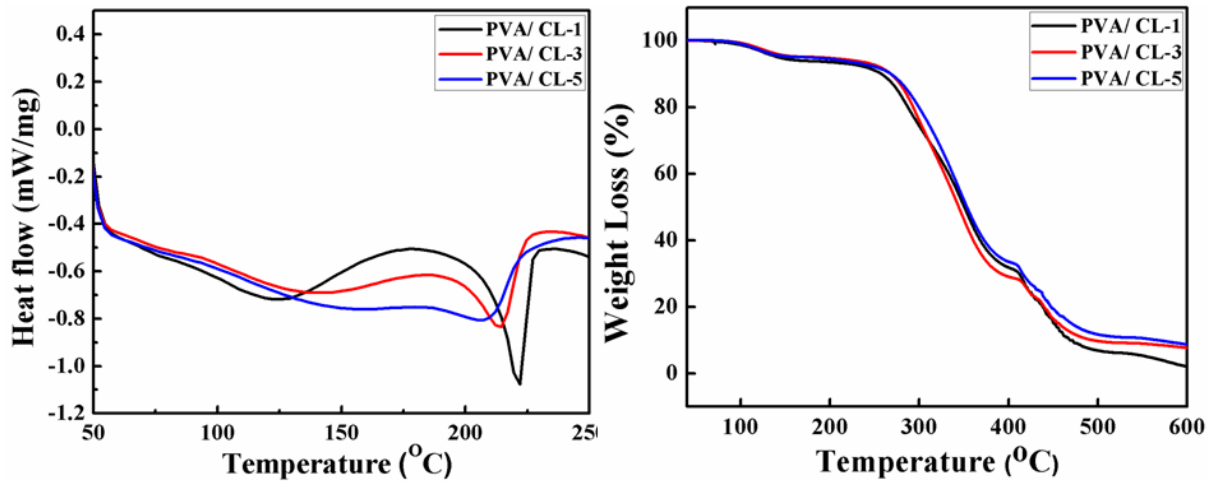


**Figure 3.6:** (a) Differential scanning calorimetry study of (i) PVA/CL-1 hydrogel (ii) PVA/CL-3 hydrogel (iii) PVA/CL-5 hydrogel.

(b) Thermo gravimetric analysis of (i) PVA/CL-1 hydrogel (ii) PVA/CL-3 hydrogel (iii) PVA/CL-5 hydrogel.

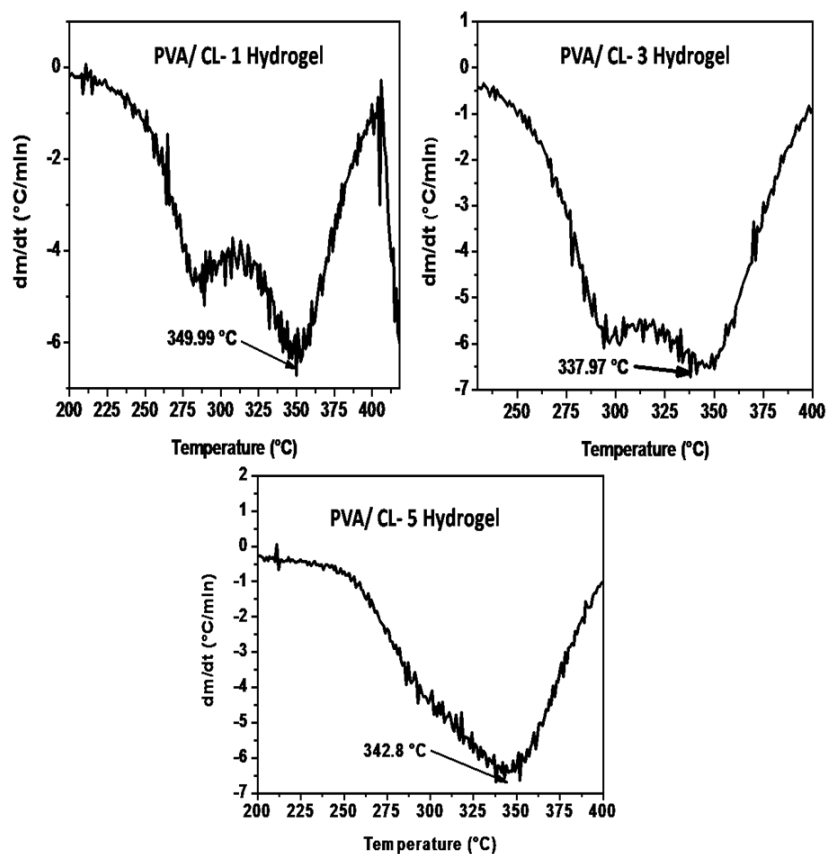


**Figure 3.7:** DTGA Study of PVA/CL Composite hydrogel.



### 3.5.2 Swelling behavior

It is important for the scaffolds, to uptake the fluid, because it influences the physical, chemical and cell loading characteristics. In other terms, the swelling has been described as the transition from an unsolvated state to a state where the pores of the hydrogel nanocomposite are swollen with fluid. Figure (3.8) shows the swelling behavior of the pure and composite hydrogels, where PVA/CL-1 and PVA/CL-5 (at the highest proportion of CL) showed the highest and lowest degree of swelling, respectively. Swelling index of hydrogels decreases with the increase of chitosan lactate concentration. In spite of the same cross-linking extent, in all the developed hydrogels, the change in swelling behavior was due to the decrease in the availability of hydrophilic functional group in the resultant hydrogel. The reduced swelling index due to the formation of crosslink rigid network by inter and intra molecular bonding simultaneously decreasing the free hydrophilic group in the hydrogels. Additionally, the glutaraldehyde accelerates crosslinking with chitosan amine group as compared to -OH group of polyvinyl alcohol. This observation is in agreement with previous studies which reported that chitosan decreases the swelling rate when mixed with PVA [43, 95, 148]. Swelling of hydrogel depends on movement of water molecules into the hydrogel network. Higher the movement of water molecules into the hydrogel, more swelling of hydrogel occurs. Swelling behaviour also depends on the mechanical strength of hydrogel. Hydrogel possess higher mechanical strength allows more movement of water molecules into their network leads to more swelling[149]. Swelling plays an important role in release of drugs from hydrogel. Swelling of hydrogel occurs after movement of water molecules into hydrogel, results into dissolution of hydrophilic drug. Afterthat, release of drug occurs through diffusion from hydrogel[150].

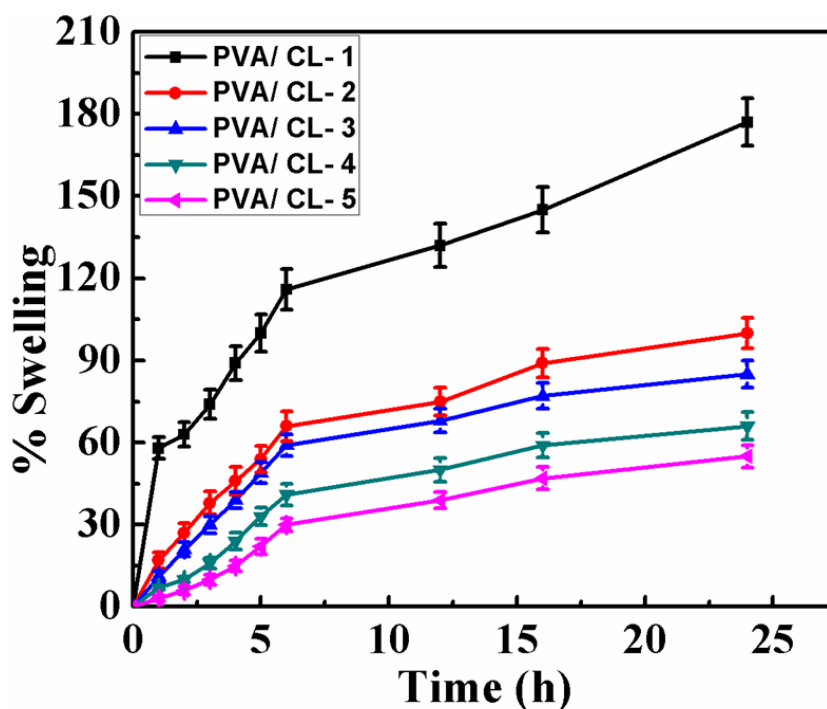


**Figure 3.8:** Swelling study of PVA/ CL based composite hydrogels.

### 3.5.3 Drug release and loading efficiency

Time-dependent drug release studies were employed to compare the ciprofloxacin release behavior of different types of drug-loaded hydrogel films as shown in Figure (3.9). The aliquot was measured using UV-Vis spectrophotometer at 270 nm. The observation of release profile of ciprofloxacin from the drug-loaded composite hydrogels shows that only 40 % of the drug was released in case of PVA/CL in about 6 h, whereas PVA hydrogel released almost all of its content. Further, in order to understand, ciprofloxacin release mechanism from the PVA/CL based composite hydrogels drug release data was fitted into Korsmeyer Pepas model to calculate the value of  $n$ [151]. The value of ‘ $n$ ’ is an indicator of the drug release mechanism for different release system. In the present study, we obtained the value of  $n$  was 0.7, 0.7, 0.6, 0.7 and 1.2 for hydrogel samples PVA/CL 1, PVA/CL 2, PVA/CL 3, PVA/CL 4, PVA/CL 5 respectively. Therefore, depending on the value of “ $n$ ”, we can conclude that PVA/CL 1,



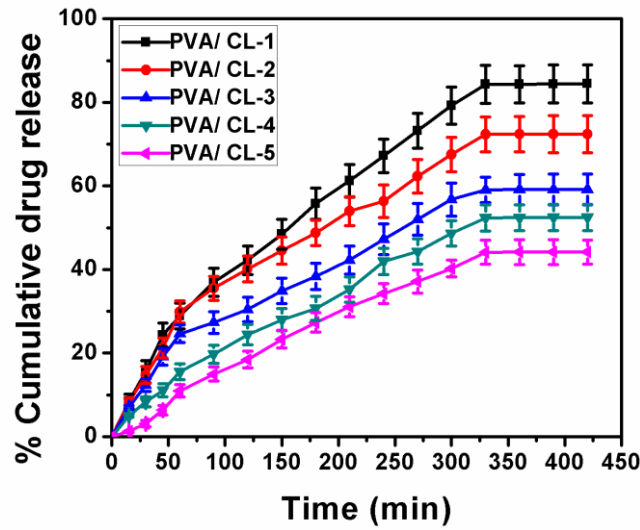


**Figure 3.9:** Ciprofloxacin drug release response of PVA/CL based composite Hydrogels.

PVA/CL 2, PVA/CL3, PVA/CL 4 show Non-Fickian diffusion mechanism whereas PVA/CL 5 shows super case II transport mechanism[151]. Release of drug from developed hydrogel occurs due to either diffusion or polymer chain relaxation. Drug release from hydrogels does not occur through the degradation of hydrogels. Since developed hydrogels does not show degradation during in-vitro degradation study. Release of drug from hydrogels occurs through diffusion or relaxation of polymer chains or both[152]. The change in the microstructures of the pores from one hydrogel composite to another is clearly reflected in the drug loading experiments. The PVA/CL-1 shows maximum drug loading due its sponge like porous structure, which reduces as we move from PVA/CL-2 to PVA/CL-5 due to pore compactness and high cross-linking. It was observed that drug loading efficiency (figure 3.10) from highest to lowest followed  $\text{PVA-CL-1} > \text{PVA-CL-2} > \text{PVA-CL-3} \approx \text{PVA-CL-4} > \text{PVA-CL-5}$ . Since each hydrogel is uniform throughout its surface, however, each hydrogel's compactness and porosity

differs from other hydrogels due to difference in their composition. Therefore, drug loading through each hydrogel occurs uniformly until 24 hours.

**Table 3.1** Release exponent (n) of PVA/ CL Hydrogel composites

| Hydrogel Sample     | PVA/ CL-1             | PVA/ CL-2             | PVA/ CL -3            | PVA/ CL -4            | PVA/ CL-5             |
|---------------------|-----------------------|-----------------------|-----------------------|-----------------------|-----------------------|
| Value of n          | 0.74                  | 0.71                  | 0.66                  | 0.75                  | 1.25                  |
| Diffusion Mechanism | Non-Fickian Diffusion | Non-Fickian Diffusion | Non-Fickian Diffusion | Non-Fickian Diffusion | SupercaseII Diffusion |

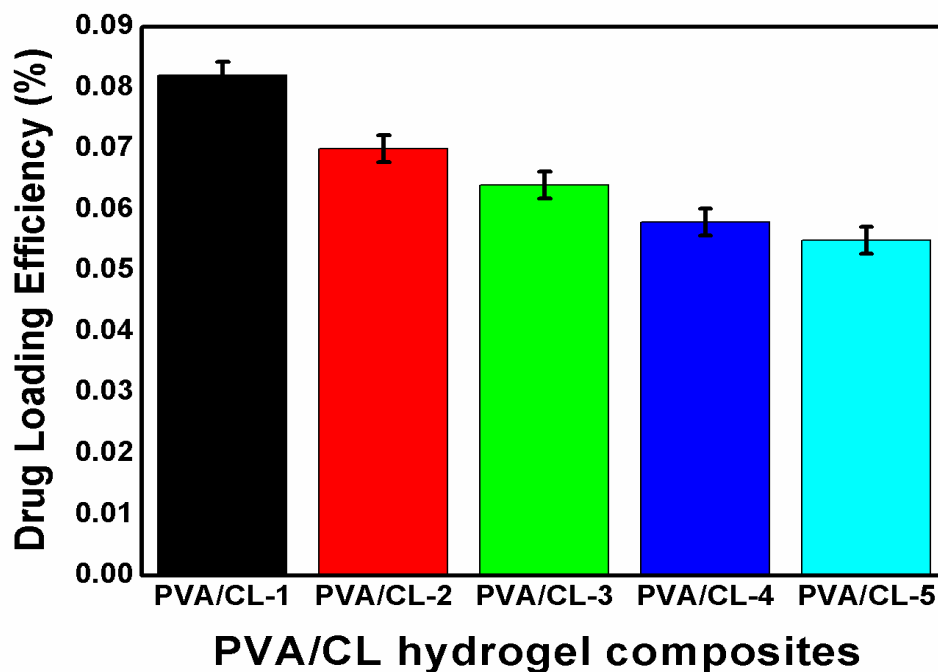


**Figure 3.10:** Ciprofloxacin drug loading efficiency of PVA/CL based composite hydrogels.

Although the drug loading efficiency of developed hydrogel composites is less. It may be due to the poor electrostatic attraction between hydrogel and loaded drug molecules. Similar work has been reported by Tronci et al. They have developed chitosan-based hydrogel using neutral and negative charged crosslinking agent. During this study, they

have functionalized Chitosan with 5-sulfoisophthalic acid monosodium salt. In this study, they have presented that positively charged drug molecules (methylene blue) shows high loading into chitosan hydrogel network. It occurs due to electrostatic attraction between covalently linked sulfonic acid moiety of chitosan and positively charged drug molecules[153].

#### **3.5.4 Antimicrobial properties**

Figure (3.11 and 3.12) shows how the application of the drug-loaded hydrogel affected the growth of *E. coli* by Agar Disc diffusion method. The entire drug-loaded hydrogel showed significantly remarkable zone of inhibition due to the release of ciprofloxacin from the hydrogel after two days, beneficial for wound healing perspective. Because, Ciprofloxacin is used as efficient antimicrobials for various applications such as eye, ear, nose and skin infections[147]. Additionally, it is important to mention that polyvinyl alcohol added chitosan lactate hydrogel without ciprofloxacin has also shown a significant zone of inhibition with the same bacteria. This might be due to the presence of chitosan lactate, which exhibits very good antibacterial property. According to Bonilla et al. (2014), the interaction of positively charged amino group with negatively charged microbial cell membranes leads the leakage of proteinaceous and intracellular constituents which enhances the antimicrobial characteristics[154].

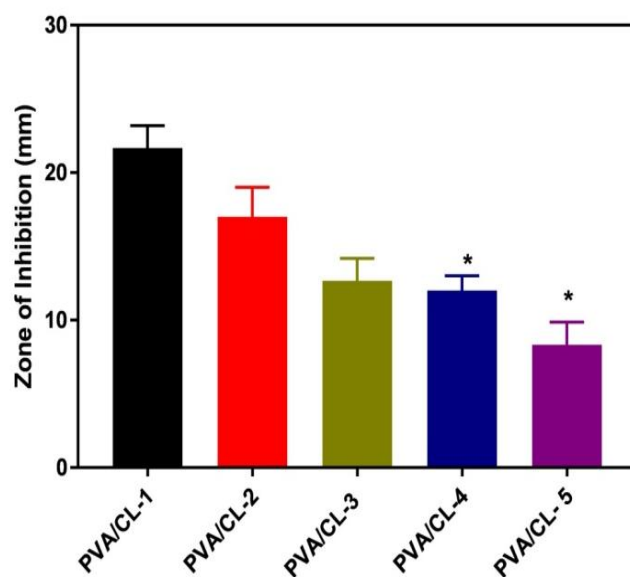


**Figure 3.11:** Zone of inhibition against E-Coli from drug loaded PVA/CL composite hydrogels.

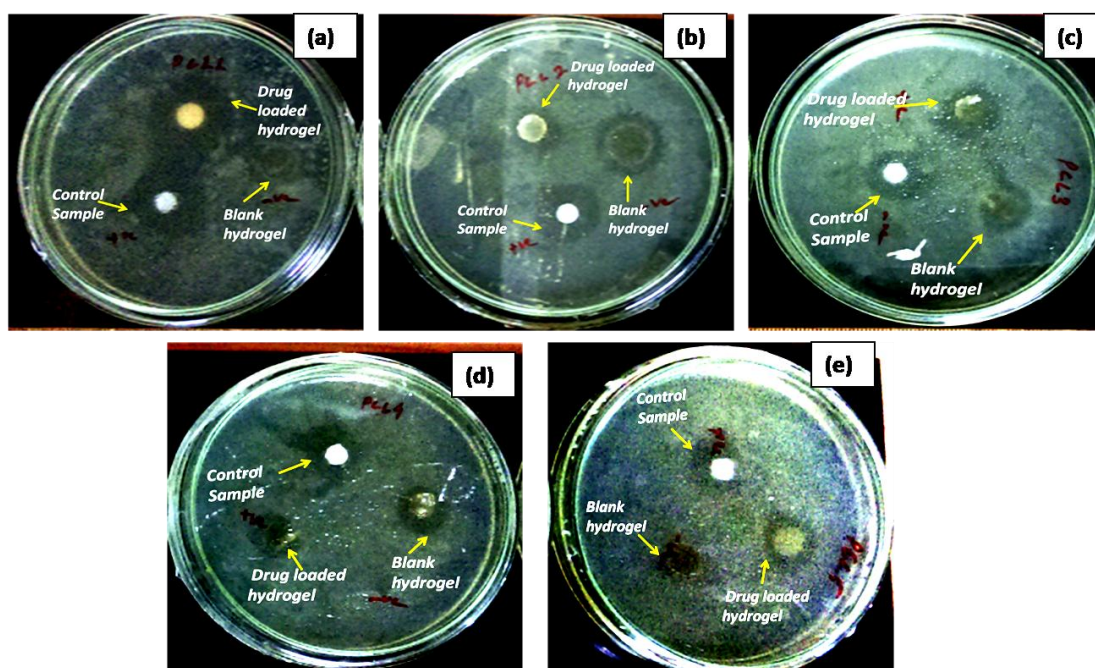


**Figure 3.12:** Picture showing Zone of Inhibition formation by PVA/ CL Composite Hydrogel.

### 3.5.5 *In vitro* cell viability and proliferation

Cellular biocompatibility of hydrogel film was measured through MTT assay and represents the active mitochondrial enzymes activity present in a cell capable of reducing MTT reagent. In this study, the viability assay was measured at 24, 48 and 72 h interval after cell seeding. The ability of the PVA/CL hydrogel film to support cell viability and proliferation shown in figure (3.13) and indicates that these samples exhibited comparable biocompatibility with mouse fibroblast (L 929 cell line). It is interesting to observe that, PVA/ CL-5 shows slight reduction in cell viability on third day with respect other hydrogel composites. This occurs due to higher compact nature of PVA/ CL-5. Due to compact surface, it resists adherence of cells on its surface[155]. But later due to swelling, loose network generated which assists in growth of cells over its surface. Beside this, highest roughness of PVA/ CL-5 also assists in growth of cells over its surface[156]. MTT results clearly revealing that the survival cells over the surface of hydrogel were more than 80%. This result shows that all the hydrogel are highly compatible with cells. It is well known that any biomaterial surface where cell survival is more than 75% is comprehensively accepted for diverse biomedical application.[157]Figure (3.14) shows the cell viability on the hydrogels after 24h. It clearly shows that increasing concentration of CL increases the viability of cells. Thus, fabricated hydrogels might be suitable for controlled drug delivery, anti-infective coatings and wound dressing.

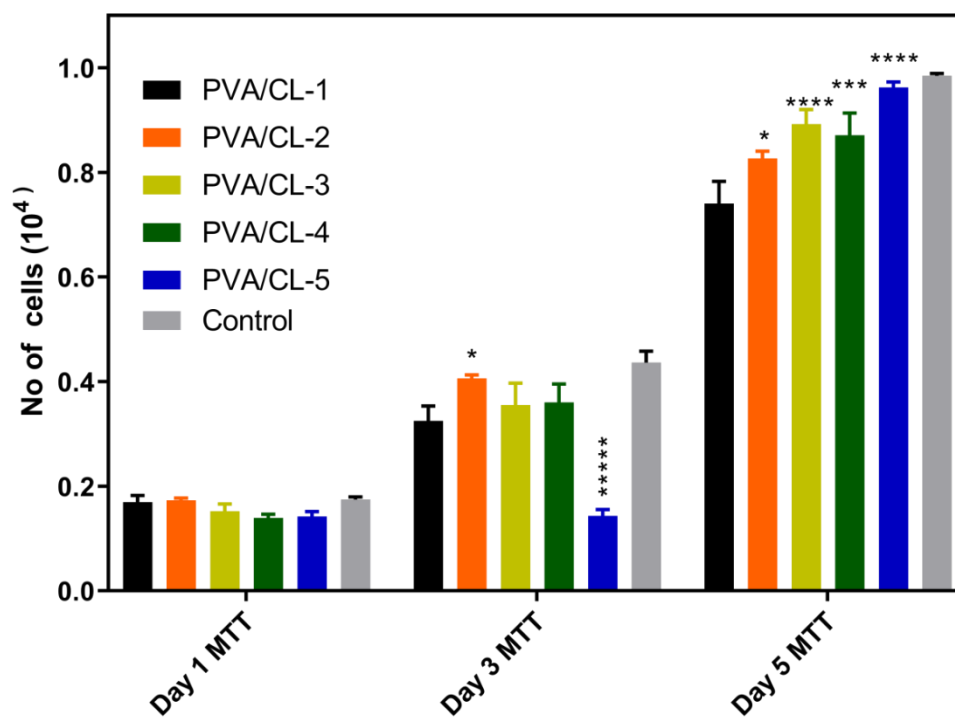


**Figure 3.13** (a) –Cytotoxicity study for PVA/ CL Composite Hydrogel.

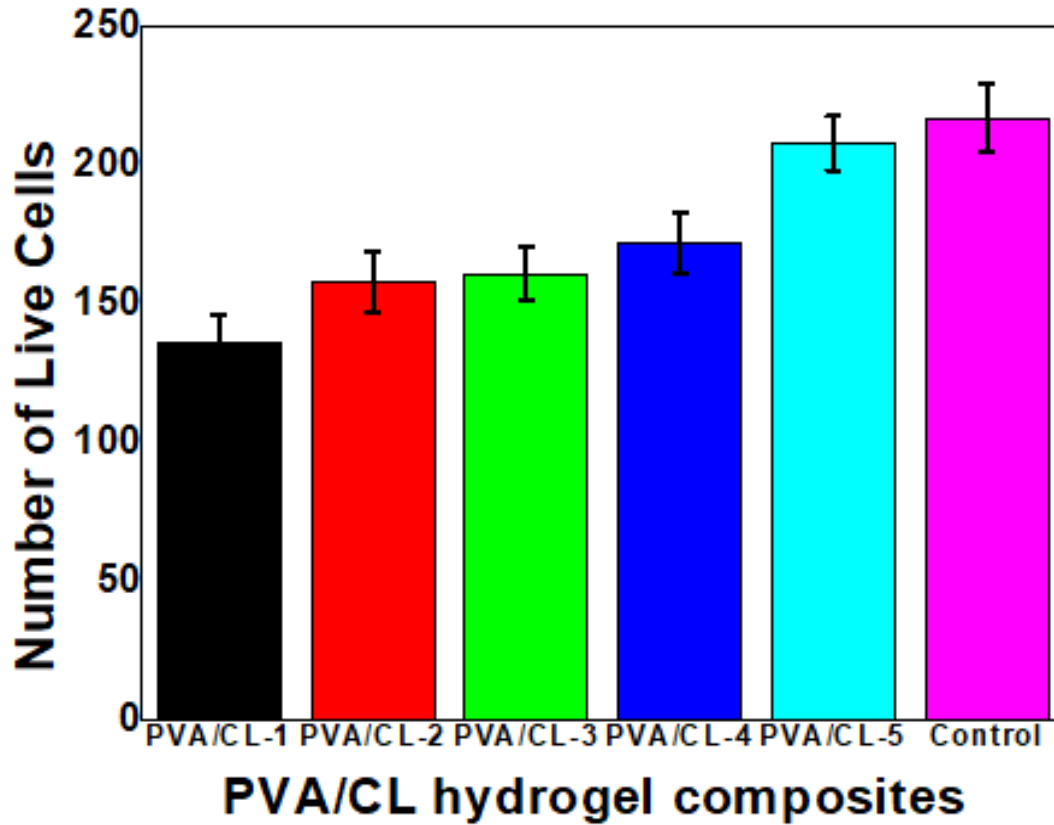


**Figure 3.13 (b)** Bar graph shows number of live cells present on each composite. Information was extracted using fluorescence images and Image J software.

### 3.5.6 In Vitro degradation study

In vitro degradation Study of all the hydrogels were performed. In vitro degradation result of all the hydrogels exhibited no loss in their mass till 96 hours. This occurs may be due to the strong crosslinking between PVA and Chitosan lactate. Due to cross linking between polymer chains, it resists its degradation in aqueous PBS (pH 7.4 ) [158]. During degradation process, dissolution of polymer takes place due to various factors such as desorption, salvation, dissociation, depolymerization of chains, hydrolysis, oxidation, reduction, diffusion, abrasion cracking, peeling and mechanical damage [133]. In the present study, due to interaction of OH group of PVA and  $\text{NH}_2$  group of Chitosan lactate, formation of covalent bond takes place between polymer chains leading to formation of strong rigid network, which is difficult to degrade in aqueous environment.

### 3.5.7 Mechanical study of hydrogel

Mechanical behavior of all the hydrogels were studied by stress relaxation test. The major parameter useful for drug delivery application is % stress relaxation. Because percentage stress relaxation provides information about viscoelastic nature. Hydrogels showing viscoelastic nature is suitable for drug delivery applications[79]. The  $\sigma_{\max}$  value of PVA/CL-1 hydrogel was found to be 1.96 Kg/ mm<sup>2</sup>. But PVA/ CL-2 hydrogel exhibited  $\sigma_{\max}$  value 2.59. This rise in  $\sigma_{\max}$  value is due to enhancement in firmness of hydrogel with the addition of chitosan lactate[128]. PVA/ CL 2 and PVA/ CL3 hydrogels shows  $\sigma_{\max}$  value 1.48 and 1.66 respectively. This decrease in  $\sigma_{\max}$  value is due to the presence of defects in the hydrogels network. It can also be explained on basis of decrease in crystallinity of hydrogel, leads to decrease in mechanical strength of the hydrogel composite network. Stress relaxation graphs of hydrogels reveals that, after attaining maximum stress value ( $\sigma_{\max}$ ), it shows exponential decay. This phenomenon is termed as stress relaxation process[128]. After completion of stress relaxation, it shows minimum stress value ( $\sigma_{\min}$ ). The  $\sigma_{\min}$  value obtained due to the elastic component of the hydrogel. The  $\sigma_{\min}$  value for PVA/CL 2 hydrogel was found to be 1.43, whereas  $\sigma_{\min}$  value for PVA/ CL-1 hydrogel was found to be 1.04. After that, decrease in  $\sigma_{\min}$  value was observed in PVA/ CL-3. The percentage stress relaxation was calculated using following equation, (3.4)-

$$\text{Stress Relaxation} = \frac{\sigma_{\max} - \sigma_{\min}}{\sigma_{\max}} * 100 \quad (3.4)$$

In the above equation,  $\sigma_{\max}$  and  $\sigma_{\min}$  represents maximum stress value (Kg/ mm<sup>2</sup>) and minimum stress value (Kg/ mm<sup>2</sup>) obtained during stress relaxation test of each specimen.

Stress relaxation value provides information about viscous component and elastic component of the sample. The 100 % stress relaxation value represents completely



viscous nature of the material, consisting viscous component only. Whereas 0 percentage stress relaxation value represents ideal elastic material[128]. In the present study stress relaxation values was found in the range of 43% to 46%, reflecting viscoelastic nature of the all the developed hydrogels. Since viscoelastic materials can hold large amount of water. Therefore, viscoelastic materials are considered as potential material for drug delivery applications [79]. Except PVA/ CL-4 hydrogels, all the remaining hydrogels shows decrease in stress relaxation value with respect to PVA/ CL-1 hydrogel. This shows increase in the elastic behavior of hydrogels, which is due to the addition of chitosan lactate. To explain stress relaxation behavior, various models has been proposed. Hooke's model is used to represent pure elastic behavior of material. Newton model is used to represent pure fluid material. But real material does not purely belong to only one of those models, but a mix of the two. To explain this behavior Weichert Model has been introduced. Weichert model possess many Maxwell elements connected in a parallel fashion[78]. Weichert model (Equation 1) was used to analyze stress relaxation of hydrogels. In this study, K1, K2, K3 represents spring constant of hydrogel. K1, K2 and K3 spring constants are related to edge, face and body directions (diagonal), respectively[159].Where, K0 represents elastic energy of the hydrogel after completion of stress relaxation test.  $\tau_1$ ,  $\tau_2$  and  $\tau_3$  represent relaxation time. Relaxation time provides information about polymeric chain interaction in hydrogel network. The quality of hydrogel is decided by % stress relaxation values. Its value should be lie between 1 to 100. If % stress relaxation values lie between 1 to 100, then it is said to be viscoelastic material. Viscoelastic materials are suitable for drug delivery applications. The model parameters such as  $K_{i \rightarrow (1 \text{ to } 3)}(K_1, K_2 \text{ \& } K_3)$ ,  $K_0$  and  $\tau_{i \rightarrow (1 \text{ to } 3)}(\tau_1, \tau_2 \text{ \& } \tau_3)$  were obtained by fitting experimental values in Weichert model [128].

$$\sigma(t) = \sum_{i=1}^n K_i \exp(-t/\tau_i) + K_0 \quad (3.5)$$

where  $\sigma(t)$  corresponds to the shear stress values as the function of time ( $\text{kg}/\text{mm}^2$ ),  $\tau_i$  is the time constants of the dashpots (sec),  $n$  corresponds to 3,  $K_i$  and  $K_0$  are the corresponding spring constant values.

$K_0$  represents the remaining elastic energy in the hydrogels after completion of stress relaxation. Relaxation time is represented by  $\tau$ . It provides useful information about polymeric chain interaction[128]. Instantaneous stress relaxation time, intermediate relaxation time and delayed relaxation time are represented by  $\tau_1$ ,  $\tau_2$  and  $\tau_3$  respectively[128]. Instantaneous stress relaxation time and intermediate relaxation time was higher for PVA/ CL-2, PVA/ CL-4 and PVA/ CL-5 with respect to PVA/ CL-1(control). This result suggests that due to addition of CL, polymer molecular arrangement process is slow in PVA/ CL composite hydrogels with respect to (control) PVA/ CL-1[128]. By fitting experimental values in Weichert model, good fitting (sum of square deviation,  $\text{SSD} < 1$ ) was obtained. Mechanical parameters were listed in table (3.2).

**Table 3.2-** Mechanical Parameters of Hydrogels

| Model                     | Parameter | PVA/ CL<br>1 | PVA/ CL<br>2 | PVA/ CL<br>3 | PVA/ CL<br>4 | PVA/ CL<br>5 |
|---------------------------|-----------|--------------|--------------|--------------|--------------|--------------|
| <b>Weichert<br/>model</b> | $K_1$     | 0.925956     | 0.756844     | 40.56918     | 0.479522     | 0.532077     |
|                           | $K_2$     | 0.358152     | 0.413314     | 0.433728     | 0.280803     | 0.31445      |
|                           | $K_3$     | 266.8644     | 48.81924     | 0.952934     | 28.66095     | 27.19251     |
|                           | $\tau_1$  | 4.273581     | 5.600451     | 0.993595     | 5.830104     | 6.182345     |
|                           | $\tau_2$  | 31.54252     | 38.62578     | 8.028813     | 40.43753     | 42.11584     |
|                           | $\tau_3$  | 0.743774     | 1.04878      | 464.9821     | 1.068103     | 1.125273     |
|                           | $K_0$     | 0.999528     | 1.397175     | 0            | 0.873616     | 1.049475     |

|   |                                 |       |       |       |       |       |
|---|---------------------------------|-------|-------|-------|-------|-------|
|   | $\sigma_{\max}(\text{kg/mm}^2)$ | 1.96  | 2.59  | 1.48  | 1.66  | 1.96  |
| - | $\sigma_{\min}(\text{kg/mm}^2)$ | 1.04  | 1.43  | 0.83  | 0.92  | 1.11  |
|   | % Stress Relaxation             | 46.93 | 44.78 | 43.91 | 44.57 | 43.36 |

Every experiment was repeated thrice for reproducibility. In this study, spring constants ( $K_1$ ,  $K_2$ ,  $K_3$ ,  $K_0$ ) and time constants ( $\tau_1$ ,  $\tau_2$ ,  $\tau_3$ ) are calculated theoretically. We have successfully added confidence interval for the measured data (stress relaxation) and also for the modelled parameter values with 95% confidence as shown in figure 3.14.

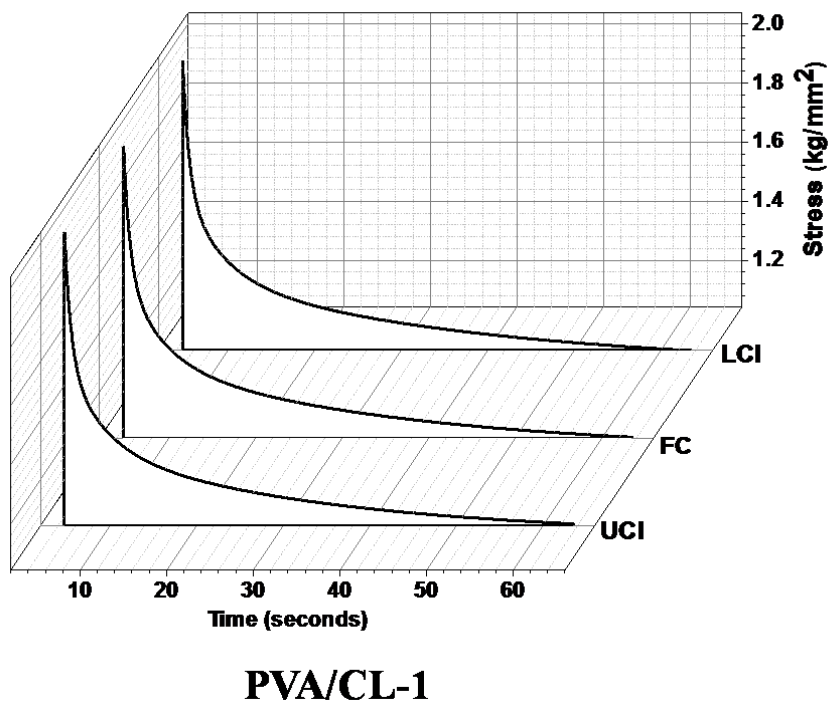
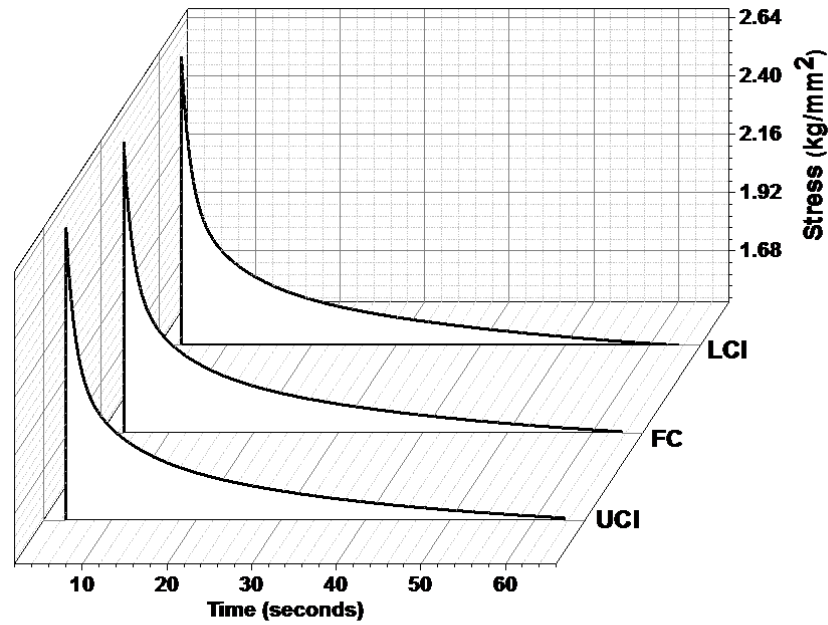
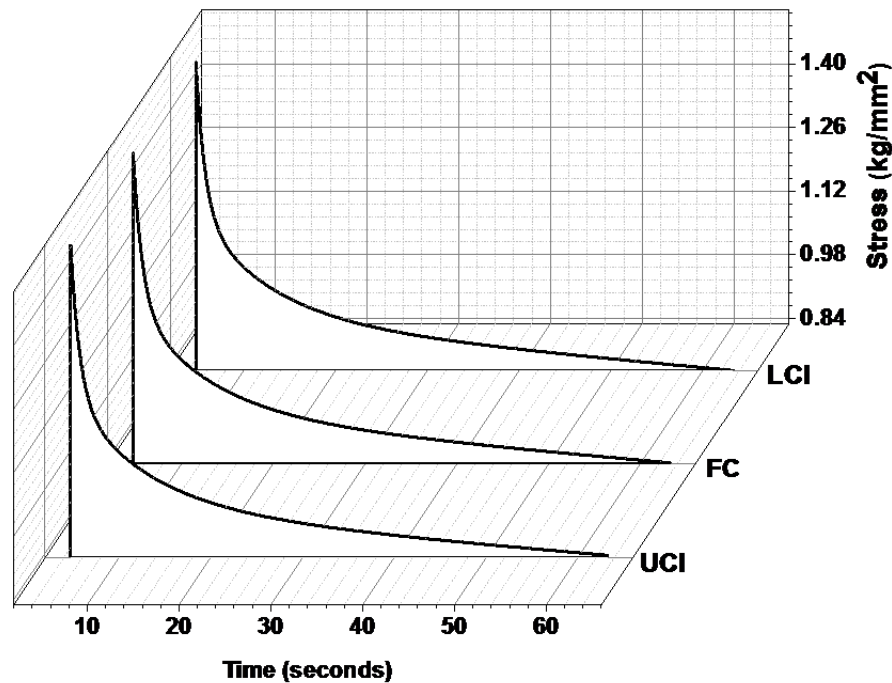


**Figure 3.14 (a):** Upper and lower values of confidence interval for the fitted curve of PVA/ CL-1 hydrogel.



### PVA/CL-2

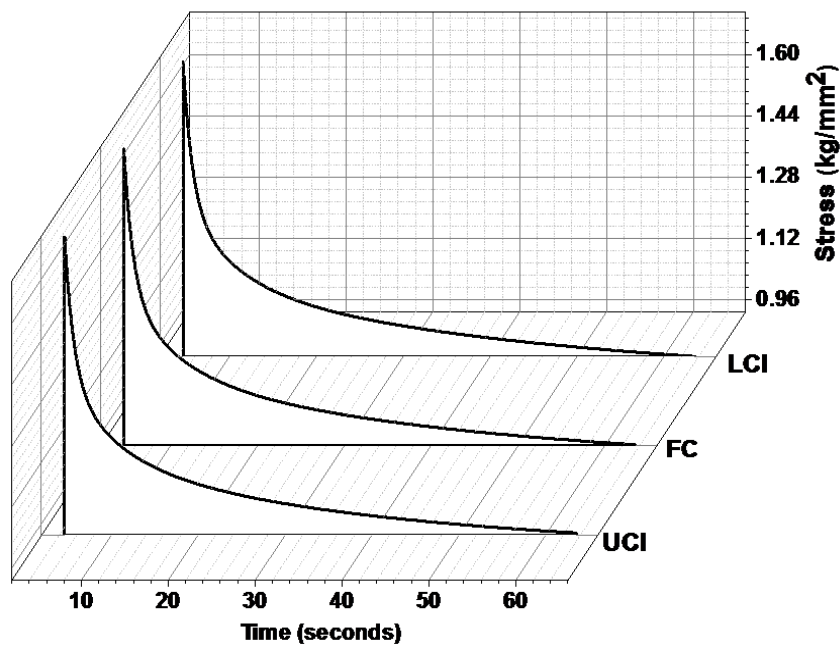
**Figure 3.14 (b):** Upper and lower values of confidence interval for the fitted curve of PVA/ CL-2 hydrogel.



### PVA/CL-3

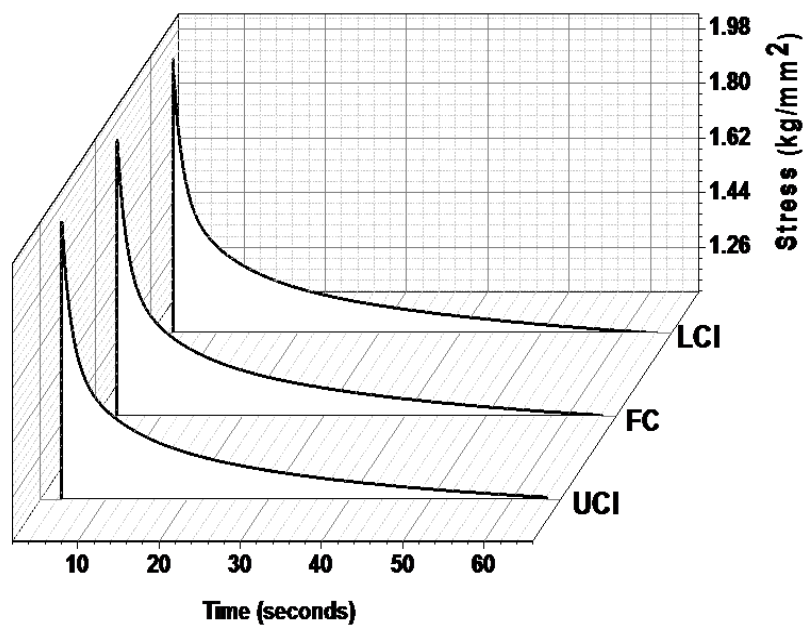
**Figure 3.14 (c):** Upper and lower values of confidence interval for the fitted curve of

PVA/ CL-3 hydrogel.



**PVA/CL-4**

**Figure 3.14 (d):** Upper and lower values of confidence interval for the fitted curve of PVA/ CL-4 hydrogel.



**PVA/CL-5**

**Figure 3.14 (e):** Upper and lower values of confidence interval for the fitted curve of PVA/ CL-5 hydrogel.

**Table 3.3-** Maximum and minimum values of confidence interval for spring constants of PVA/ CL-1 hydrogel.

| Constants | PVA/ CL-1  |            |            |
|-----------|------------|------------|------------|
|           | Minimum CI | Model      | Maximum CI |
| $K_1$     | 0.92578239 | 0.92595598 | 0.92613207 |
| $K_2$     | 0.35769337 | 0.35815177 | 0.35861674 |
| $K_3$     | 266.864365 | 266.864366 | 266.864366 |
| $\tau_1$  | 4.27353909 | 4.27358134 | 4.27362418 |
| $\tau_2$  | 31.5425162 | 31.542517  | 31.5425178 |
| $\tau_3$  | 0.74182746 | 0.74377383 | 0.74570258 |
| $K_0$     | 0.99899417 | 0.9995279  | 1.0000693  |

**Table 3.4-** Maximum and minimum values of confidence interval for spring constants of PVA/ CL-2 hydrogel.

| Constants | PVA/CL-2    |           |             |
|-----------|-------------|-----------|-------------|
|           | Minimum CI  | Model     | Maximum CI  |
| $K_1$     | 0.756300744 | 0.7568436 | 0.757391205 |
| $K_2$     | 0.412208549 | 0.4133143 | 0.414429732 |
| $K_3$     | 48.8192286  | 48.819243 | 48.81925769 |
| $\tau_1$  | 5.600389758 | 5.6004508 | 5.600512291 |
| $\tau_2$  | 38.6257746  | 38.625776 | 38.62577746 |

|          |             |           |             |
|----------|-------------|-----------|-------------|
| $\tau_3$ | 1.04574622  | 1.0487799 | 1.051797177 |
| $K_0$    | 1.395927807 | 1.3971753 | 1.3984338   |

**Table 3.5-** Maximum and minimum values of confidence interval for spring constants of PVA/ CL-3 hydrogel.

| Constants | PVA/CL-3    |             |             |
|-----------|-------------|-------------|-------------|
|           | Minimum CI  | Model       | Maximum CI  |
| $K_1$     | 40.5691745  | 40.56918361 | 40.56919265 |
| $K_2$     | 0.43310826  | 0.433728024 | 0.43435075  |
| $K_3$     | 0.95182174  | 0.952934288 | 0.954052164 |
| $\tau_1$  | 0.99179707  | 0.993594612 | 0.995382438 |
| $\tau_2$  | 8.02879312  | 8.028813051 | 8.028833022 |
| $\tau_3$  | 464.982106  | 464.9821064 | 464.9821065 |
| $K_0$     | -0.00112404 | 0           | 0.001129427 |

**Table 3.6-** Maximum and minimum values of confidence interval for spring constants of PVA/ CL-4 hydrogel.

| Constants | PVA/CL-4    |          |            |
|-----------|-------------|----------|------------|
|           | Minimum CI  | Model    | Maximum CI |
| $K_1$     | 0.478844757 | 0.479522 | 0.4802029  |
| $K_2$     | 0.279461354 | 0.280803 | 0.2821531  |
| $K_3$     | 28.66092813 | 28.66095 | 28.660966  |
| $\tau_1$  | 5.830059468 | 5.830104 | 5.8301486  |

|          |             |          |           |
|----------|-------------|----------|-----------|
| $\tau_2$ | 40.43752426 | 40.43753 | 40.437526 |
| $\tau_3$ | 1.065857401 | 1.068103 | 1.0703406 |
| $K_0$    | 0.872110916 | 0.873616 | 0.8751314 |

**Table 3.7-** Maximum and minimum values of confidence interval for spring constants of PVA/ CL-5 hydrogel.

| Constants | PVA/CL-5   |          |            |
|-----------|------------|----------|------------|
|           | Minimum CI | Model    | Maximum CI |
| $K_1$     | 0.53131587 | 0.532077 | 0.532844   |
| $K_2$     | 0.31300482 | 0.31445  | 0.315904   |
| $K_3$     | 27.1924794 | 27.19251 | 27.19253   |
| $\tau_1$  | 6.18229611 | 6.182345 | 6.182395   |
| $\tau_2$  | 42.1158412 | 42.11584 | 42.11584   |
| $\tau_3$  | 1.12267082 | 1.125273 | 1.127867   |
| $K_0$     | 1.04786175 | 1.049475 | 1.051099   |

Percentage stress relaxation of hydrogel was computed using maximum and minimum stress relaxation values. For each hydrogel (PVA/CL-1, PVA/CL-2, PVA/CL-3, PVA/CL-4, PVA/CL-5) the calculated maximum and minimum values of stress relaxation are different, which resulted to different values of percentage relaxation. The individual % stress relaxation values for PVA/CL-1, PVA/CL-2, PVA/CL-3, PVA/CL-4, PVA/CL-5 is 46.93, 44.78, 43.91, 44.57, and 43.36 respectively. We have successfully calculated Confidence Interval for percentage relaxation with 95% confidence. Since, these values



are within 95% confidence limit the % stress relaxation values, are statistically significant.

We have calculated lower and upper confidence intervals for percentage stress relaxation of PVA hydrogel network based on modelled (theoretical) values.

**Table 3.8-** Upper and lower values of confidence interval for  $\sigma_{\max}$  and  $\sigma_{\min}$  of PVA/ CL hydrogel composites.

| Sample   | ( $\sigma_{\max}$ )<br>LCI | $\sigma_{\max}$ | ( $\sigma_{\max}$ )<br>UCI | ( $\sigma_{\min}$ )<br>LCI | $\sigma_{\min}$ | ( $\sigma_{\min}$ )<br>UCI |
|----------|----------------------------|-----------------|----------------------------|----------------------------|-----------------|----------------------------|
| PVA/CL-1 | 2.020                      | 2.028           | 2.036                      | 1.043                      | 1.047           | 1.051                      |
| PVA/CL-2 | 2.657                      | 2.666           | 2.676                      | 1.471                      | 1.477           | 1.482                      |
| PVA/CL-3 | 1.507                      | 1.512           | 1.518                      | 0.828                      | 0.831           | 0.834                      |
| PVA/CL-4 | 1.698                      | 1.704           | 1.711                      | 0.928                      | 0.931           | 0.935                      |
| PVA/CL-5 | 2.015                      | 2.022           | 2.030                      | 1.113                      | 1.117           | 1.122                      |

**Table 3.9-** Upper and lower values of confidence interval for % stress relaxation of PVA/ CL hydrogel composites.

| Sample   | (% $\sigma$ )<br>LCI | % $\sigma$ | (% $\sigma$ )<br>UCI |
|----------|----------------------|------------|----------------------|
| PVA/CL-1 | 47.958               | 48.370     | 48.779               |
| PVA/CL-2 | 44.203               | 44.613     | 45.020               |
| PVA/CL-3 | 44.608               | 45.005     | 45.399               |
| PVA/CL-4 | 44.916               | 45.326     | 45.733               |
| PVA/CL-5 | 44.317               | 44.727     | 45.134               |

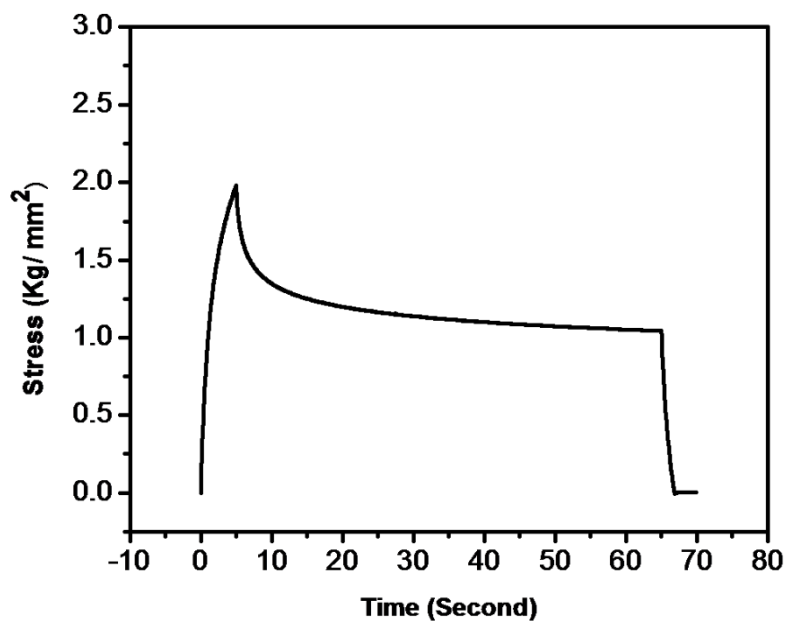


**Figure 3.15 (a):** Stress Relaxation graph of PVA/ CL-1 Hydrogel.

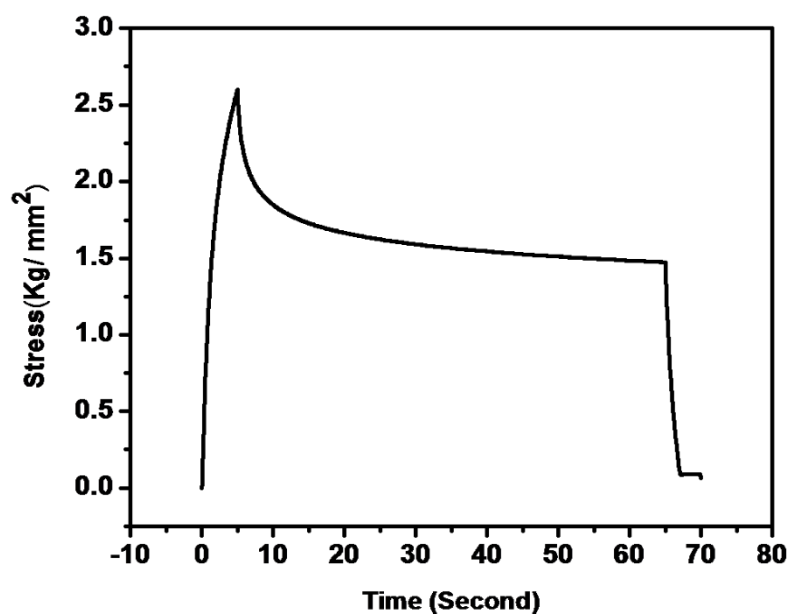


**Figure3.15 (b):** Stress Relaxation graph of PVA/ CL-2 Hydrogel.

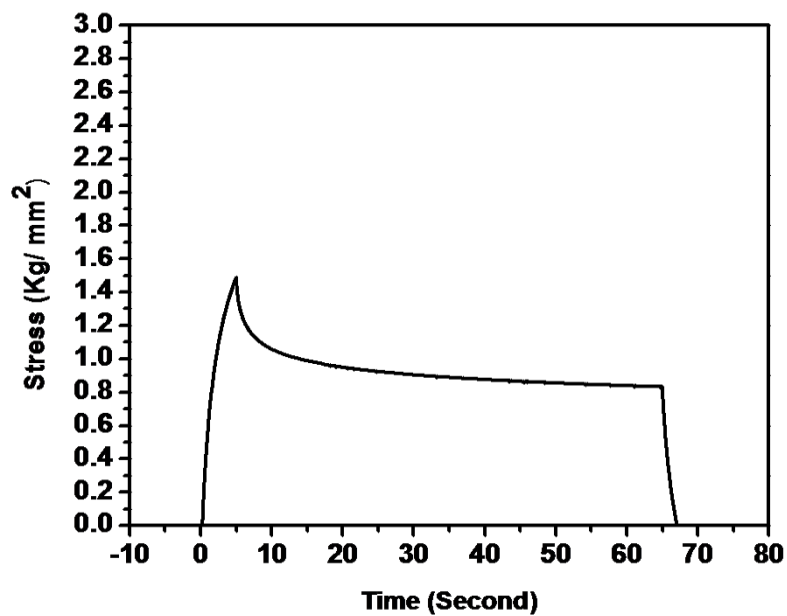


Figure 3.15 (c): Stress Relaxation graph of PVA/ CL-3 Hydrogel.

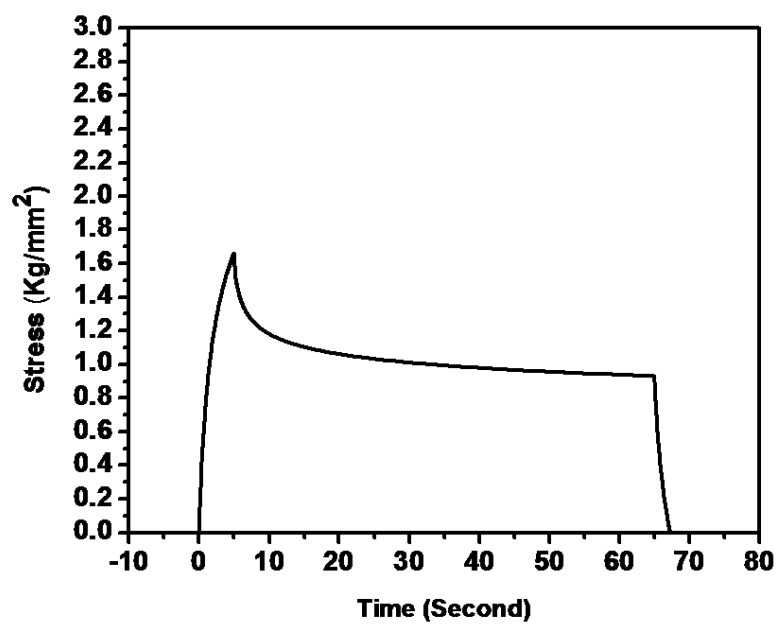


Figure3.15 (d): Stress Relaxation graph of PVA/ CL-4 Hydrogel.

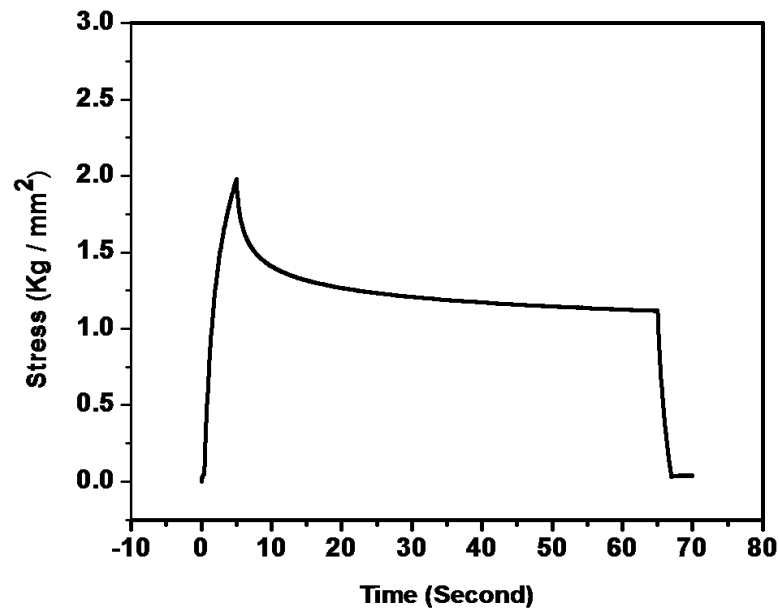


Figure 3.15 (e): Stress Relaxation graph of PVA/ CL-5 Hydrogel.

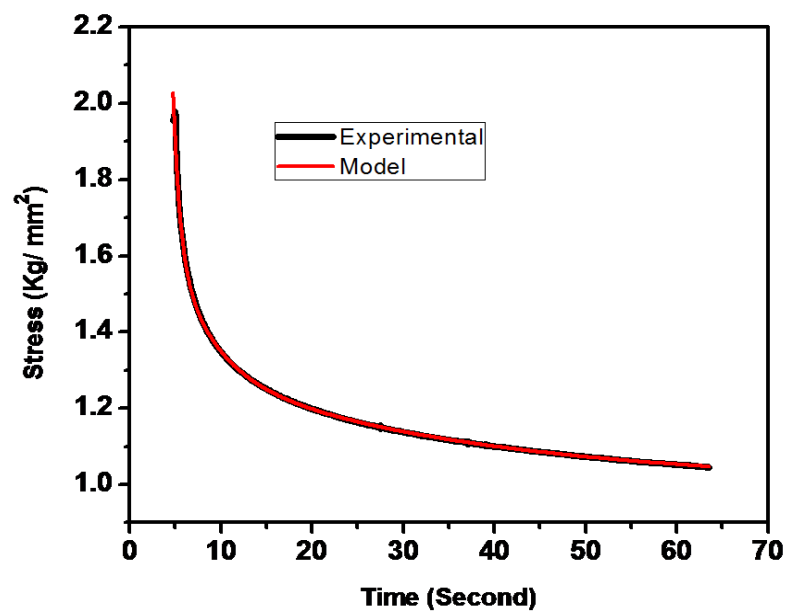
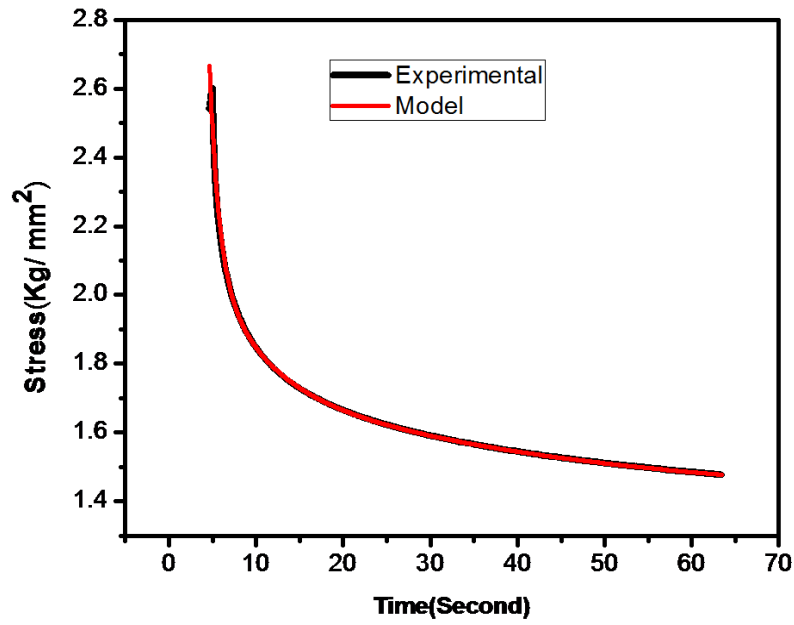
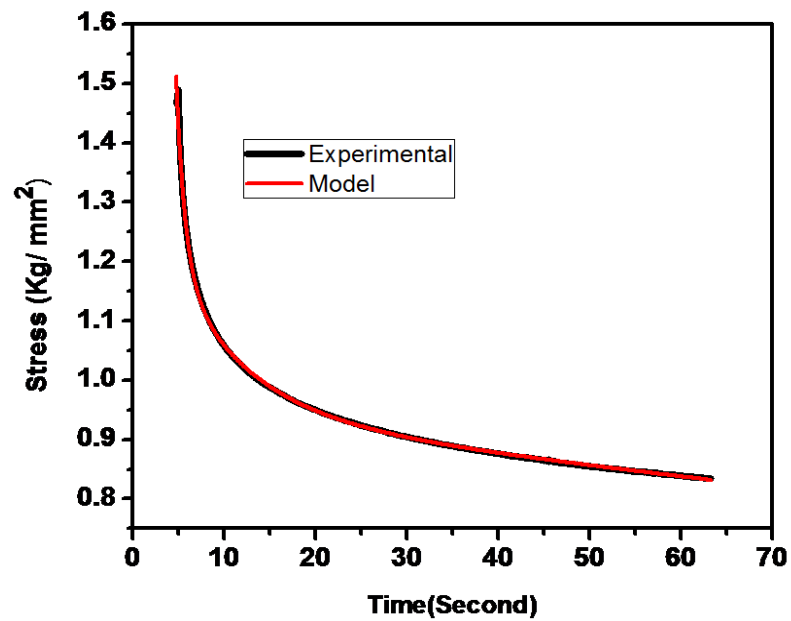


Figure 3.16 (a): Comparison of Stress relaxation experimental result and modeling of PVA/ CL-1 hydrogel.



**Figure 3.16 (b)** Comparison of Stress relaxation experimental result and modeling of PVA/ CL-2 hydrogel.



**Figure 3.16 (c):** Comparison of Stress relaxation experimental result and modeling of PVA/ CL-3 hydrogel.

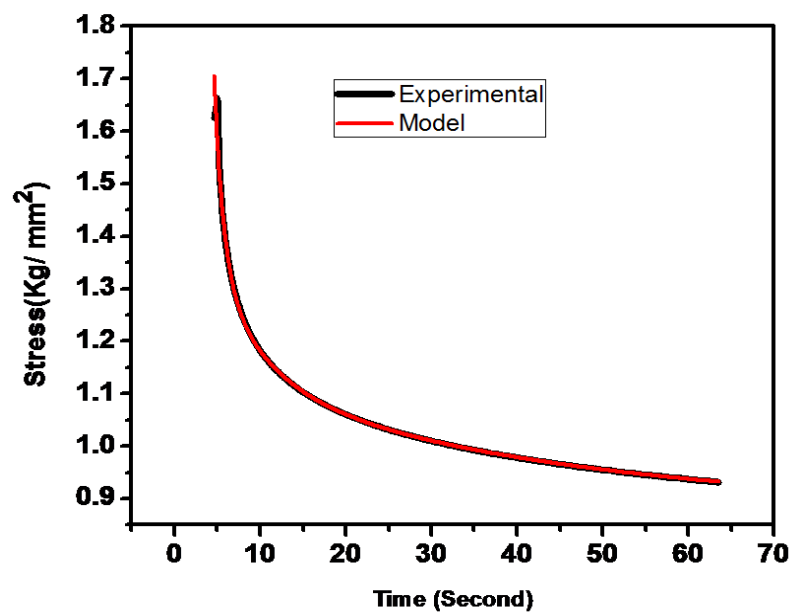


**Figure 3.16 (d):** Comparison of Stress relaxation experimental result and modeling of PVA/ CL-4 hydrogel.

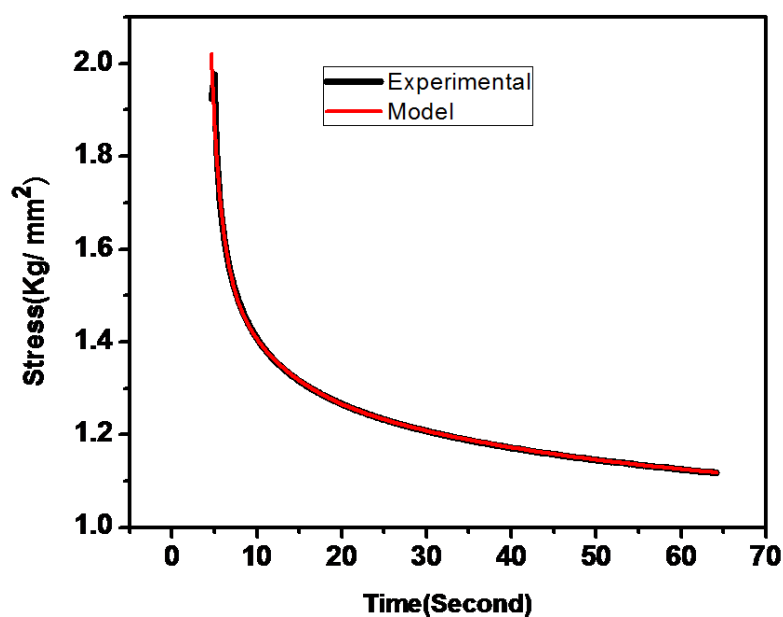


**Figure 3.16 (e):** Comparison of Stress relaxation experimental result and modeling of PVA/ CL-5 hydrogel.

### 3.5.8 Contact angle evaluation of hydrogel

Contact angle of all hydrogel samples were determined by plate method. Contact angle of PVA/ CL-1 hydrogel sample was found to be highest ( $72^{\circ}$ ). Whereas, contact angle of PVA/ CL -5 hydrogel sample was found to be lowest ( $62^{\circ}$ ). From this study, it was found that contact angle of hydrogel sample decreases with increase in the concentration of Chitosan lactate. Contact angle provides information about hydrophilicity and hydrophobicity. By estimating contact angle of a material, we can acquire information about cell adhesion. The contact angle range for proper growth of fibroblast should be  $60^{\circ}$  to  $80^{\circ}$ [160]. Based on this observation, it can be concluded that hydrophilicity of the composite hydrogel increases with addition of Chitosan lactate[161].

### 3.6 Conclusion

Polyvinyl alcohol and chitosan lactate based composite hydrogels were synthesized by the chemical cross-linking method. We achieved improved thermal properties and suitable surface roughness by increasing the concentration of chitosan lactate. Increase in chitosan lactate concentration was also allowed us to control the ciprofloxacin released from the hydrogel. This sustained release of ciprofloxacin further inhibited the growth of *E. coli* which was grown in petri plate. *In vitro* cell viability against L929 cells show that the fabricated hydrogels are compatible with cells. From MTT results, we can propose that prepared hydrogels may be used for various biomedical applications. Cell viability was further evaluated by fluorescent dye acridine orange and ethidium bromide. Thus, we anticipate the improved properties of the fabricated composite hydrogels can be used for biomedical applications.